

PPAR α activity is impaired in mice deficient for the circadian PAR bZip transcription factors DBP, HLF, and TEF

Frédéric Gachon^{1, 2}, Nicolas Leuenberger^{3, 6}, Thierry Claudel⁴, Pascal Gos¹, Céline Jouffe², Fabienne Fleury Olela¹, Xavier de Mollerat du Jeu⁵, Walter Wahli³ and Ueli Schibler¹

¹Department of Molecular Biology, National Center of Competence in Research “Frontiers in Genetics”, Sciences III, University of Geneva, Geneva 4, CH-1211, Switzerland

²Department of Pharmacology and Toxicology, University of Lausanne, Lausanne, CH-1005, Switzerland

³Center for Integrative Genomics, National Center of Competence in Research “Frontiers in Genetics”, University of Lausanne, Lausanne, CH-1015, Switzerland

⁴Laboratory of Experimental and Molecular Hepatology, Division of Gastroenterology and Hepatology, Department of Medicine, Medical University Graz, Graz, A-8036, Austria

⁵Life Technologies, Carlsbad, California 92008, USA

⁶Present address: Swiss Laboratory for Doping Analysis, Epalinges, CH-1066, Switzerland

Contacts:

Frédéric Gachon
Department of Pharmacology and Toxicology
University of Lausanne
Rue du Bugnon, 27
CH-1005 Lausanne
Switzerland

Tel: (00 41) 21 692 53 64
Fax: (00 41) 21 692 53 55

E-mail: Frederic.Gachon@unil.ch

Ueli Schibler
Department of Molecular Biology
University of Geneva
30 quai Ernest-Ansermet
1211 Genève 4
Switzerland

Tel: (00 41) 22 379 61 75
Fax: (00 41) 22 379 68 68

E-mail: ueli.schibler@unige.ch

ABSTRACT

In mammals, many aspects of metabolism are under circadian control. At least in part, this regulation is achieved by core-clock or clock-controlled transcription factors whose abundance and/or activity oscillate during the day. The clock-controlled PAR domain basic leucine zipper (PAR bZip) proteins DBP, TEF and HLF have previously been shown to participate in the circadian control of xenobiotic detoxification in liver and other peripheral organs. Here we present genetic and biochemical evidence that the three PAR bZip proteins also play a key role in circadian lipid metabolism by influencing the rhythmic expression and activity of the nuclear receptor PPAR α . Our results suggest that in liver, DBP, HLF, and TEF contribute to the circadian transcription of genes specifying acyl-CoA thioesterases (ACOTs), leading to a cyclic release of fatty acids (FA) from thioesters. In turn the FA act as ligands for PPAR α , and the activated PPAR α receptor then stimulates the transcription of genes encoding proteins involved in the uptake and/or metabolism of lipids, cholesterol, and glucose metabolism.

Keywords: PAR bZip transcription factors; circadian clock; liver lipid metabolism; peroxisome proliferator activated receptor α (PPAR α).

\body

In mammals, energy homeostasis demands that anabolic and catabolic processes are coordinated with alternating periods of feeding and fasting. There is increasing evidence that inputs from the circadian clock are required in addition to acute regulatory mechanisms to adapt metabolic functions to an animal's daily needs. For example, mice with disrupted hepatocyte clocks display a hypoglycemia during the postabsorptive phase, supposedly because hepatic gluconeogenesis and glucose delivery into the bloodstream are dysregulated in these animals (1).

The regulation of lipid metabolism is also governed by an interaction between acute and circadian regulatory mechanisms, and the three peroxisome proliferator activated receptors (PPAR α , PPAR β/δ , and PPAR γ) play particularly important roles in these processes (2). Among them, PPAR α acts as a molecular sensor of endogenous fatty acids (FA) and regulates the transcription of genes involved in lipid uptake and catabolism. Moreover, it accumulates according to a daily rhythm and reaches maximal levels around the beginning of feeding time (3, 4). For liver and many other peripheral tissues, feeding-fasting rhythms are the most dominant *Zeitgebers* (timing cues) (5, 6). This observation underscores the importance of the crosstalk between metabolic and circadian cycles.

Circadian oscillators in peripheral tissues can participate in the control of rhythmic metabolism through circadian transcription factors, which in turn regulate the cyclic transcription of metabolically relevant downstream genes. The three PAR-domain basic leucine zipper (PAR bZip) proteins DBP, TEF, and HLF are examples of such output mediators (for review, see 7). Mice deficient of only one or two members of the PAR bZip gene family display rather mild phenotypes, suggesting that the three members execute partially redundant functions. However, mice deficient of all three PAR bZip genes

(henceforth called PAR bZip 3KO mice) have a dramatically reduced life span, due to epileptic seizures (8) and impaired xenobiotic detoxification (9).

Genome-wide transcriptome profiling of wild-type and PAR bZip 3KO mice has revealed differentially expressed genes involved in lipid metabolism, many of which are targets of the nuclear receptor PPAR α . Here we present evidence for a pathway in which PAR bZip transcription factors connect the accumulation and activity of PPAR α to circadian oscillators in liver.

RESULTS

***Ppar* α expression in PAR bZip 3KO mice**

Genome-wide microarray transcriptome profiling studies with liver RNA from wild-type and PAR bZip 3KO mice revealed differentially expressed genes involved in xenobiotic detoxification (9) and lipid metabolism (this paper). The latter included *Ppar* α , a gene specifying a nuclear receptor that is well known as a regulator of lipid metabolism, and many PPAR α target genes (10) (Figure S1A). We validated the reduced accumulation of *Ppar* α mRNA and transcripts issued by PPAR α target genes by using quantitative RT-PCR analysis (Figure 1A, 1B and S1B). The examined PPAR α target genes include *Cyp4a10* and *Cyp4a14*, encoding enzymes involved in mitochondrial fatty acid ω -oxidation (whose expression is strongly reduced in *Ppar* α KO mice, see Figure S2A), and genes specifying enzymes involved in fatty acid β -oxidation (Figure S1B). PPAR α has also been shown to activate transcription from its own promoter, when activated by PPAR α agonists (11). To evaluate the relevance of this feed-forward loop in circadian *Ppar* α transcription, we compared the temporal expression of *Ppar* α pre-mRNA in the liver of wild-type mice with that of non-productive pre-mRNA transcripts issued by the disrupted *Ppar* α alleles in *Ppar* α KO mice

(12). As depicted in Figure 1C, the circadian expression was indeed dampened in these animals, suggesting that PPAR α contributed to the rhythmic transcription of its own gene. Therefore, PAR bZip transcription factors may have activated *Ppar α* transcription through an indirect mechanism, for example by promoting the cyclic generation of PPAR α ligands.

Unexpectedly, hepatic PPAR α protein accumulation was higher in PAR bZip 3KO mice as compared to wild-type mice, in spite of the lower mRNA levels in the former (Figure 1D). However, nuclear receptors can be destabilized in a ligand-dependent manner (for review, see 13). Hence, the higher protein to mRNA level in hepatocytes of PAR bZip 3KO mice could indicate that in these animals PPAR α was less active and therefore more stable than in the liver of wild-type mice. To examine this conjecture, we measured hepatic PPAR α protein and mRNA accumulation, four hours after an intraperitoneal injection of the synthetic PPAR α ligand WY14643 into PAR bZip 3KO mice. As shown in Figure 1E and Figure S3, the injection of the PPAR α ligand led to a decrease of the protein to mRNA ratio, in keeping with the model of Kamikaze activators postulated by Thomas and Tyers (14). The lower PPAR α protein to mRNA ratio in wild-type as compared to PAR bZip 3KO mice may therefore indicate that PPAR α had a higher activity in the former animals than in the latter.

PAR bZip transcription factors may stimulate PPAR α activity through the production of PPAR α ligands

FA generated by the metabolism of dietary lipids or *de novo* synthesis are the best known natural ligands for PPAR α (15-17). In liver, FA can be produced through the hydrolysis of acyl-CoAs by ACOTs (18) and through the hydrolysis of lipids in lipoproteins by lipoprotein lipases (LPLs) (19). Interestingly, members of both of these two enzyme families have been reported to accumulate according to a daily rhythm in the liver (20-22), and our genome wide

transcriptome profiling experiments suggested that the mRNAs for these enzymes were expressed at reduced levels in PAR bZip 3KO mice. As shown in Figure 2B, the accumulation of transcripts specifying ACOTs displayed temporal expression patterns expected for direct PAR bZip target genes and was indeed blunted in PAR bZip 3KO mice. The *Acot* genes are all located on a 120 kb cluster on mouse chromosome 12, and a perfect PAR bZip DNA binding sequence is located between *Acot1* and *Acot4* (Figure 2A). At least *in vitro*, this sequence binds PAR bZip in a diurnal manner (Figure 2A), and this could explain the rhythmic expression of these genes. However, the phase of *Lpl* transcript accumulation was found to be delayed by 12 hrs when compared to that of *Acot* expression, and we suspected that PAR bZip proteins regulate *Lpl* transcription *via* an indirect mechanism. Interestingly, *Acot* and *Lpl* reached maximal concentrations at ZT12 and ZT24, respectively, suggesting a bimodal metabolism of FA in mouse liver: hydrolysis of acyl-CoAs at the day-night transition and hydrolysis of lipids in lipoproteins at the night-day transition.

The transcription of *Acots* and *Lpl* has previously been reported to be regulated by PPAR α (21-23), and the expression of these genes, in addition to that of *Cyp4a10* and *Cyp4a14*, is activated by injection of WY14643 (Figure S4). We thus decided to examine the role of PPAR α on their diurnal expression by comparing liver RNAs harvested around the clock from *Ppar α* KO and wild-type mice. As shown in Figure S2B, the overall expression levels of *Acots* were only slightly decreased in *Ppar α* KO animals for *Acot3* and *Acot4*, not changed for *Acot2*, but 2.5 fold increased for *Acot1*. However, zenith levels were reached about 4 to 12 hours later in *Ppar α* KO as compared to wild-type mice. All in all the changes of *Acot* and *Lpl* expression in PPAR α deficient mice were complex and reflected perhaps a synergistic regulation by PAR bZip transcription factors and PPAR α or other transcription factors.

In the absence of food-derived lipids PPAR α ligands can also be generated *de novo* by synthesis of FA by fatty acid synthase (FASN) (24, 25). Interestingly, *Fasn* expression was enhanced in PAR bZip 3KO animals, perhaps to compensate for the deficient import and/or metabolism of lipids absorbed with the food. Perhaps for the same reasons, the expression of *Fabp1* and *Cd36*, genes encoding proteins involved in fatty acid transport and uptake, was also increased in these mice (Figure S1B). As described previously (26), *Fasn* expression was decreased in the liver of *Ppar α* KO mice, probably reflecting a perturbed activation of the sterol-response element binding protein (SREBP) in these animals (27).

The downregulation of *Acot* expression reduces the activity of PPAR α target genes

Our results insinuated that PAR bZip proteins may stimulate the activity of PPAR α indirectly. According to this scenario, PAR bZip proteins govern the expression of the ACOT isoforms 1 to 4, which in turn liberate fatty acids from acyl coA thioesters that may serve as PPAR α ligands. In order to examine this possibility, the hepatic expression of ACOTs 1 to 4 was downregulated by the injection of siRNAs into the tail vein (for experimental details, see Supporting Informations and Figure S9). As shown in Figures 2C and S9, a decrease in ACOT2, ACOT3, and ACOT4 expression was sufficient to specifically inhibit the expression of the PPAR α target genes *Cyp4a10* and *Cyp4a14*, confirming the role of ACOTs in the activation of PPAR α . Likewise, the intravenous application of an equimolar mixture of ACOT1-4 siRNAs specifically reduced the accumulation of *Cyp4a10* and *Cyp4a14* mRNAs (Figures 2C and S9).

The impaired activity of PPAR α in the liver of PAR bZip 3KO mice may be due to a deficiency of fatty acids

The results presented in the previous section suggested that the downregulation of ACOTs and LPL in PAR bZip 3KO mice may have caused a decrease in the levels of hepatic FA that can serve as PPAR α ligands. We thus measured the levels of various FA in the livers of wild-type and PAR bZip 3KO mice. In the former, the concentrations of all examined FA displayed a robust circadian fluctuation with a maximum at ZT12 (Figure 3A, grey columns). In addition, a second, but smaller peak was observed for most of the FA. This bimodal distribution was consistent with the hypothesis that the temporal expression of ACOTs and LPL (see Figure 2) were responsible for the hepatic accumulation of FA. In PAR bZip 3KO mice, the FA levels were low throughout the day (Figure 3A, white columns). Again, these results were compatible with a downregulation of ACOTs and LPL in PAR bZip 3KO mice (Figure 2B). Importantly, several of the examined FA had previously been identified as PPAR α ligands. For example, C18:1, C18:2 and C18:3 appear to be particularly potent PPAR α ligands (15-17, 28), and the decrease in these FA probably accounted for the downregulation of PPAR α target genes in PAR bZip 3KO animals. The blunted activation of the PPAR α pathway in PAR bZip 3KO mice would be expected to manifest itself in a broad dysregulation of hepatic metabolism and associated changes in blood chemistry (26, 29). As depicted in Figure 3B, PAR bZip 3KO mice showed indeed an increase in the serum concentrations of cholesterol, triglyceride and glucose, similar to the observations made with *Ppar α* knockout mice.

PAR bZip 3KO mice have an impaired capacity to adapt to caloric restriction

A large number of genes induced by fasting are direct or indirect target genes of PPAR α (30, 31), and *Ppar α* KO mice have indeed difficulties in adapting to caloric restriction (29, 32-36). If the activation of the PPAR α signaling was inhibited in PAR bZip 3KO mice, one would expect that these animals would also have an impaired capacity to adjust their

metabolism to reduced food availability. In order to test this hypothesis, we exposed PAR bZip 3KO mice to a feeding regimen in which the quantity of food was reduced to 60% of what these mice absorbed when food was offered *ad libitum*. As shown in Figure S5, PAR bZip 3KO mice subjected to this regimen suffered from a rapid and dramatic weight loss, as compared to wild-type mice. However this difference could not be attributed to a difference in energy expenditure, as O₂ consumption and CO₂ production were nearly identical in wild-type and PAR bZip 3KO animals (Figure S6). We also compared the food anticipatory activities (FAA) of wild-type and PAR bZip 3KO mice (Figure S7A-B). FAA manifests itself in the onset of enhanced locomotor activity (wheel-running) a few hours before the time when food becomes available. When food availability was limited to a 6-hour time span between ZT03 to ZT09, PAR bZip 3KO mice displayed exacerbated FAA and actually shifted a large fraction of their wheel-running activity to this time window during the light phase. As expected, wild-type mice did show FAA but kept running the wheel mainly during the dark phase. These results suggested that the activity associated with food searching equaled or even dominated SCN-driven locomotor activity in PAR bZip 3KO animals when food availability became limiting. Since PPAR α KO mice did not show enhanced FAA (Figure S7C), the exacerbated FAA cannot have been caused solely by the impaired PPAR α activity in PAR bZip 3KO mice.

PPAR α ligands can be generated from food-derived and *de novo* synthesized lipids

As discussed above, FA PPAR α ligands can be generated from diet-derived lipids or *de novo* synthesis by fatty acid synthase (FASN), and the first pathway appeared to be deficient in PAR bZip 3KO mice. We wished to determine the expression of putative PPAR α target genes and genes with key functions in the production of PPAR α ligands in wild-type and PAR bZip 3KO mice that were fed with a fat-free diet during an extended time span (5

weeks). Under these conditions, FA can be produced exclusively through *de novo* synthesis. As shown in Figure 4A, the PPAR α target genes *Cyp4a10* and *Cyp4a14* mRNAs accumulated to similar levels in wild-type and PAR bZip 3KO mice receiving a fat-free diet, unlike of what had been observed in animals fed on normal chow. The similar expression of this PPAR α target gene in mice receiving a fat-free diet suggested that *de novo* synthesis of FA serving as PPAR α agonists was not affected by the absence PAR bZip transcription factors, and *Fasn* mRNA was indeed expressed at similar concentrations in wild-type and PAR bZip 3KO mice receiving fat-free food. Hence, the fat-free diet rescued the deficiency of PPAR α activity in PAR bZip 3KO mice, presumably because *de novo* synthesis of FA in liver did not depend upon pathways requiring the circadian PAR bZip proteins. This interpretation was validated by our observation that the hepatic concentrations of various FA in wild-type and PAR bZip were similar in wild-type and PAR bZip 3KO mice exposed to a fat-free diet (Figure S8). Interestingly, the expression of *Ppar α* and *Acots* was also rescued by the fat-free diet in PAR bZip 3KO mice, and in keeping with earlier observations (11, 21, 22) both of these genes were indeed activated by PPAR α ligands. *Lpl* expression did not exhibit large differences between mice fed with normal and fat-free chow. Similarly, blood glucose, cholesterol, and triglyceride levels were not significantly different between wild-type and PAR bZip 3KO mice kept on a fat-free diet (Figure 4B), unlike of what we have observed for animals fed with normal chow.

DISCUSSION

The PAR bZip transcription factors DBP, HLF, and TEF regulate circadian PPAR α activity.

Here we present evidence for a novel clock output pathway operative in hepatocytes, which connects the PAR bZip transcription factors DBP, HLF, and TEF to the circadian activity of

PPAR α . This nuclear receptor has long been known to play a key role in the coordination of lipid metabolism, and like several other nuclear receptors it accumulates in a circadian manner (3, 4). Our studies revealed that *Ppar α* mRNA levels were reduced in PAR bZip 3KO mice. However, PPAR α protein accumulated to higher than wild-type levels in these animals, presumably due to its reduced transactivation potential.

Our gene expression studies, combined with hepatic FA measurements, offered a plausible biochemical pathway for the PAR bZip-dependent activation of PPAR α , schematized in Figure 5. PAR bZip proteins drive directly or indirectly the expression of *Acots* and *Lpl*, which in turn release FA from acyl-coA thioesters and lipoproteins, respectively. FA then serve as ligands of PPAR α and initiate a feed-forward loop, in which PPAR α enhances transcription from its own gene. This scenario is supported by our observation that the siRNA-mediated dampening of *Acot2*, *Acot3*, and *Acot4* expression led to a downregulation of the expression of *Cyp4a10* and *Cyp4a14*, two bonafide target genes of PPAR α .

The accumulation cycles of *Acots* and *Lpl* mRNA had widely different phases; yet both were strongly attenuated in PAR bZip 3KO mice. While the phase of *Acot* expression was compatible with that expected for direct PAR bZip target genes, *Lpl* mRNA reached maximal levels at a time (ZT24) when all three PAR bZip proteins were expressed at nadir values. We thus suspect that *Lpl* transcription was controlled by a complex pathway, in which the precise roles of PPAR α and PAR bZip proteins remain to be clarified. The temporal accumulation of most determined FA revealed a major peak at ZT12, when *Acots* were maximally expressed, and a minor peak at ZT24, when *Lpl* was maximally expressed. The control of FA catabolism through β -oxidation and lipid uptake are major functions of PPAR α . On first sight the low hepatic FA levels in PAR bZip 3KO mice, in which PPAR α activity appeared to be blunted, was perhaps surprising. However, this apparent conundrum

can be rationalized as follows. Free FA are natural ligands for PPAR α , and a minimal FA threshold concentration may thus be required for the activation of PPAR α (15-17, 28). Moreover, acyl-CoA esters antagonize the activation of PPAR α by free FA (37, 38). Since, due to the reduced expression of *Acots* in PAR bZip 3KO mice, these esters were probably less efficiently hydrolyzed, the ratio of free FA to acyl-CoA esters is expected to be lower in these animals as compared to wild-type mice. The attenuation of PPAR α activity in the PAR bZip 3KO mice is expected to be associated with an impaired uptake of FA from the blood (39-41).

PPAR α expression has first been found to follow a daily rhythm by Lemberger *et al.*, (3). Subsequently, Oishi *et al.* (42) demonstrated that the core clock transcription factor CLOCK is required for circadian *Ppar α* transcription and that CLOCK binds to a series of E-box sequences within the first intron. This might explain why PPAR α expression is still circadian in PAR bZip 3KO mice, albeit with reduced amplitude and magnitude.

PPAR α target gene expression is rescued in PAR bZip 3KO mice fed with a fat-free diet

In animals kept on a fat-free diet hepatic FA synthesis is strongly induced (43). We thus suspected that the intracellular availability of FA rescued PPAR α mediated transcription in PAR bZip 3KO mice. Indeed, the production of mRNAs encoding enzymes implicated in FA synthesis, such as FASN, was strongly induced in wild-type and PAR bZip 3KO mice receiving fat-free diet. Furthermore, in contrast to mice fed on a normal chow, PAR bZip 3KO and wild-type animals fed on a fat-free diet accumulated similar hepatic levels of mRNAs specified by *Ppar α* , and the putative PPAR α target genes *Cyp4a10* and *Cyp4a14*. We did notice, however, that *Acot* expression, whose overall magnitude was only slightly changed in PPAR α KO mice, was also rescued in PAR bZip 3KO mice kept on a fat-free diet. Hence, as previously suggested (21, 22), *Acot* transcription was also augmented by

PPAR α , but probably required high concentrations of natural ligands (i.e. FA). It is noteworthy that 1-palmitoyl-2-oleoyl-*sn*-glycerol-3-phosphocholine (16:0/18:1-GPC), whose FASN-dependent synthesis was activated under a fat free diet, has recently been discovered as a highly potent PPAR α ligand (24).

PAR bZip 3KO mice are unable to adapt to restricted feeding

Wild-type mice exposed to caloric restriction lost about 13 % of their body mass during the first three weeks and then kept their mass within narrow boundaries over several months. In contrast, PAR bZip 3KO animals rapidly lost more than 20 % of their weight and had to be euthanized after about a week, since they probably would have succumbed to wasting after this time period. At least in part, the failure of PAR bZip deficient mice may be due to a decreased PPAR α activity, as *Ppar α* KO mice have been reported to adapt poorly to calorie restriction (29, 32-36). However, not all phenotypes of PAR bZip 3KO mice related to feeding could be assigned to an impaired PPAR α activity. Thus, in contrast to PAR bZip 3KO mice, *Ppar α* KO mice did not exhibit an exacerbated food anticipatory activity (FAA).

The capacity to adapt activity and metabolism to feeding-fasting cycles is primary to an animal's health and survival, and the disruption of the circadian timing system has indeed been linked to obesity and other metabolic disorders (44-46).

EXPERIMENTAL PROCEDURES

Animal housing conditions

All animal studies were conducted in accordance with the regulations of the veterinary office of the State of Geneva and of the State of Vaud. PAR bZip 3KO mice with disrupted *Dbp*, *Tef* and *Hlf* genes (8) and mice with *Ppar α* null alleles (12) have been described previously. Mice were maintained under standard animal housing conditions, with free access to food and water, and a 12h light/12h dark cycle. Specific treatments and feeding regimens are described in Supporting Informations.

Blood chemistry

Blood samples were harvested after decapitation of the animals, and sera were obtained by centrifugation of coagulated samples for 10 minutes at 4500 rpm at room temperature. The sera were stored at -20°C until analyzed. Triglycerides and total cholesterol were measured using commercially available enzymatic kits according to the manufacturer's instructions (Triglyceride; Cholesterol; Roche/Hitachi Mannheim GmbH, Mannheim, Germany). Glucose was measured using the glucose oxidase method adapted to rodent (GO assay kit Sigma-Aldrich, Handels GmbH, Wien, Austria).

Liver fatty acids measurement:

Mouse livers were homogenized in 0.5 ml of phosphate buffered saline and 0.5 ml of methanol. This procedure inhibits triglycerides lipases and allows their elimination. Each sample was immediately spiked with 50 nmol of 15:0 FA as an internal standard. Subsequently, lipids were extracted according to Bligh and Dyer (47) and fatty acids were then measured by GC-MS as described in Supplemental Information.

RNA isolation and analysis

Livers were removed within 4 min after decapitation, frozen in liquid nitrogen, and stored at -70°C until use. The extraction of whole-cell RNA and its analysis by real-time RT-PCR were conducted as described previously (8). The values were normalized to those obtained for *Gapdh* mRNA. Sequences of the oligonucleotides used are given in Supplemental Information.

Preparation of nuclear protein extracts and Western blotting

Liver nuclear proteins were prepared by using the NaCl-Urea-NP40 (NUN) procedure (48). Western blotting was carried out as described (9). The rabbit anti-PPAR α and murine anti-U2AF⁶⁵ antibodies were purchased from Cayman chemical (Ann Arbor, MI) and Sigma (St. Louis, MO), respectively.

ACKNOWLEDGEMENTS

We thank Nicolas Roggli for the artwork, and Joel Gyger and Bernard Thorens from the Mouse Metabolic Facility (MEF) of the University of Lausanne for indirect calorimetry experiments. This research was supported by the Swiss National Science Foundation (through individual research grants to U.S., W.W., and F.G., and the National Center of Competence in Research Program Frontiers in Genetics to U.S. and W.W.), the Cantons of Geneva and Vaud, the Louis Jeantet Foundation of Medicine, the Bonizzi-Theler-Stiftung (to U.S. and W.W.), and the 6th European Framework Project EUCLOCK (to U.S.).

REFERENCES

1. Lamia KA, Storch K-F, & Weitz CJ (2008) Physiological significance of a peripheral tissue circadian clock. *Proc Natl Acad Sci U S A.* 105(39):15172-15177.
2. Desvergne B, Michalik L, & Wahli W (2006) Transcriptional Regulation of Metabolism. *Physiol. Rev.* 86(2):465-514.
3. Lemberger T, *et al.* (1996) Expression of the Peroxisome Proliferator-activated Receptor α Gene Is Stimulated by Stress and Follows a Diurnal Rhythm. *J. Biol. Chem.* 271(3):1764-1769.
4. Yang X, *et al.* (2006) Nuclear Receptor Expression Links the Circadian Clock to Metabolism. *Cell* 126(4):801-810.
5. Damiola F, *et al.* (2000) Restricted feeding uncouples circadian oscillators in peripheral tissues from the central pacemaker in the suprachiasmatic nucleus. *Genes Dev.* 14(23):2950-2961.
6. Stokkan K-A, Yamazaki S, Tei H, Sakaki Y, & Menaker M (2001) Entrainment of the Circadian Clock in the Liver by Feeding. *Science* 291(5503):490-493.
7. Gachon F (2007) Physiological function of PARbZip circadian clock-controlled transcription factors. *Ann Med.* 39(8):562 - 571.
8. Gachon F, *et al.* (2004) The loss of circadian PAR bZip transcription factors results in epilepsy. *Genes Dev.* 18(12):1397-1412.
9. Gachon F, Fleury Olela F, Schaad O, Descombes P, & Schibler U (2006) The circadian PAR-domain basic leucine zipper transcription factors DBP, TEF, and HLF modulate basal and inducible xenobiotic detoxification. *Cell Metab.* 4(1):25-36.
10. Leuenberger N, Pradervand S, & Wahli W (2009) Sumoylated PPAR α mediates sex-specific gene repression and protects the liver from estrogen-induced toxicity in mice. *J Clin Invest* 119(10):3138-3148.

11. Pineda Torra I, Jamshidi Y, Flavell DM, Fruchart J-C, & Staels B (2002) Characterization of the Human PPAR α Promoter: Identification of a Functional Nuclear Receptor Response Element. *Mol Endocrinol*. 16(5):1013-1028.
12. Lee SS, *et al.* (1995) Targeted disruption of the α isoform of the peroxisome proliferator-activated receptor gene in mice results in abolishment of the pleiotropic effects of peroxisome proliferators. *Mol Cell Biol*. 15(6):3012-3022.
13. Rochette-Egly C (2005) Dynamic Combinatorial Networks in Nuclear Receptor-mediated Transcription. *J. Biol. Chem*. 280(38):32565-32568.
14. Thomas D & Tyers M (2000) Transcriptional regulation: Kamikaze activators. *Curr Biol* 10(9):R341-R343.
15. Forman BM, Chen J, & Evans RM (1997) Hypolipidemic drugs, polyunsaturated fatty acids, and eicosanoids are ligands for peroxisome proliferator-activated receptors α and δ . *Proc Natl Acad Sci U S A*. 94(9):4312-4317.
16. Kliewer SA, *et al.* (1997) Fatty acids and eicosanoids regulate gene expression through direct interactions with peroxisome proliferator-activated receptors α and γ . *Proc Natl Acad Sci U S A*. 94(9):4318-4323.
17. Krey G, *et al.* (1997) Fatty Acids, Eicosanoids, and Hypolipidemic Agents Identified as Ligands of Peroxisome Proliferator-Activated Receptors by Coactivator-Dependent Receptor Ligand Assay. *Mol Endocrinol* 11(6):779-791.
18. Hunt MC & Alexson SEH (2002) The role Acyl-CoA thioesterases play in mediating intracellular lipid metabolism. *Prog Lipid Res*. 41(2):99-130.
19. Ziouzenkova O, *et al.* (2003) Lipolysis of triglyceride-rich lipoproteins generates PPAR ligands: Evidence for an antiinflammatory role for lipoprotein lipase. *Proc Natl Acad Sci U S A*. 100(5):2730-2735.

20. Benavides A, Siches M, & Llobera M (1998) Circadian rhythms of lipoprotein lipase and hepatic lipase activities in intermediate metabolism of adult rat. *Am J Physiol.* 275(3):R811-817.
21. Hunt MC, *et al.* (2000) Involvement of the peroxisome proliferator-activated receptor α in regulating long-chain acyl-CoA thioesterases. *J. Lipid Res.* 41(5):814-823.
22. Hunt MC, Solaas K, Kase BF, & Alexson SEH (2002) Characterization of an Acyl-CoA Thioesterase That Functions as a Major Regulator of Peroxisomal Lipid Metabolism. *J. Biol. Chem.* 277(2):1128-1138.
23. Schoonjans K, *et al.* (1996) PPAR α and PPAR γ activators direct a distinct tissue-specific transcriptional response via a PPRE in the lipoprotein lipase gene. *EMBO J.* 15(19):5336-5348.
24. Chakravarthy MV, *et al.* (2009) Identification of a Physiologically Relevant Endogenous Ligand for PPAR α in Liver. *Cell* 138(3):476-488.
25. Chakravarthy MV, *et al.* (2005) "New" hepatic fat activates PPAR α to maintain glucose, lipid, and cholesterol homeostasis. *Cell Metab.* 1(5):309-322.
26. Patel DD, Knight BL, Wiggins D, Humphreys SM, & Gibbons GF (2001) Disturbances in the normal regulation of SREBP-sensitive genes in PPAR α -deficient mice. *J. Lipid Res.* 42(3):328-337.
27. Knight BL, *et al.* (2005) A role for PPAR α in the control of SREBP activity and lipid synthesis in the liver. *Biochem J* 389(2):413-421.
28. Lin Q, Ruuska SE, Shaw NS, Dong D, & Noy N (1998) Ligand Selectivity of the Peroxisome Proliferator-Activated Receptor α . *Biochemistry* 38(1):185-190.
29. Hashimoto T, *et al.* (2000) Defect in Peroxisome Proliferator-activated Receptor α - inducible Fatty Acid Oxidation Determines the Severity of Hepatic Steatosis in Response to Fasting. *J. Biol. Chem.* 275(37):28918-28928.

30. Bauer M, *et al.* (2004) Starvation response in mouse liver shows strong correlation with life-span-prolonging processes. *Physiol. Genomics* 17(2):230-244.
31. Corton JC, *et al.* (2004) Mimetics of Caloric Restriction Include Agonists of Lipid-activated Nuclear Receptors. *J. Biol. Chem.* 279(44):46204-46212.
32. Badman MK, *et al.* (2007) Hepatic Fibroblast Growth Factor 21 Is Regulated by PPAR α and Is a Key Mediator of Hepatic Lipid Metabolism in Ketotic States. *Cell Metab.* 5(6):426-437.
33. Inagaki T, *et al.* (2007) Endocrine Regulation of the Fasting Response by PPAR α -Mediated Induction of Fibroblast Growth Factor 21. *Cell Metab.* 5(6):415-425.
34. Kersten S, *et al.* (1999) Peroxisome proliferator-activated receptor α mediates the adaptive response to fasting. *J. Clin. Invest.* 103(11):1489-1498.
35. Lee SST, *et al.* (2004) Requirement of PPAR α in maintaining phospholipid and triacylglycerol homeostasis during energy deprivation. *J. Lipid Res.* 45(11):2025-2037.
36. Leone TC, Weinheimer CJ, & Kelly DP (1999) A critical role for the peroxisome proliferator-activated receptor α (PPAR α) in the cellular fasting response: The PPAR α -null mouse as a model of fatty acid oxidation disorders. *Proc Natl Acad Sci U S A.* 96(13):7473-7478.
37. Elholm M, *et al.* (2001) Acyl-CoA Esters Antagonize the Effects of Ligands on Peroxisome Proliferator-activated Receptor α Conformation, DNA Binding, and Interaction with Co-factors. *J. Biol. Chem.* 276(24):21410-21416.
38. Jørgensen C, *et al.* (2002) Opposing Effects of Fatty Acids and Acyl-CoA Esters on Conformation and Cofactor Recruitment of Peroxisome Proliferator-Activated Receptors. *Ann N Y Acad Sci.* 967:431-439.
39. Bremer J (2001) The biochemistry of hypo- and hyperlipidemic fatty acid derivatives: metabolism and metabolic effects. *Prog Lipid Res.* 40(4):231-268.

40. Fruchart J-C & Duriez P (2006) Mode of action of fibrates in the regulation of triglyceride and HDL-cholesterol metabolism. *Drugs Today* 42(1):39-64.
41. Martin G, Schoonjans K, Lefebvre A-M, Staels B, & Auwerx J (1997) Coordinate Regulation of the Expression of the Fatty Acid Transport Protein and Acyl-CoA Synthetase Genes by PPAR α and PPAR γ Activators. *J. Biol. Chem.* 272(45):28210-28217.
42. Oishi K, Shirai H, & Ishida N (2005) CLOCK is involved in the circadian transactivation of peroxisome-proliferator-activated receptor α (PPAR α) in mice. *Biochem. J.* 386:575–581.
43. Towle HC, Kaytor EN, & Shih H-M (1997) Regulation of the expression of lipogenic enzyme genes by carbohydrate. *Annu Rev Nutr.* 17(1):405-433.
44. Buijs RM & Kreier F (2006) The Metabolic Syndrome: A Brain Disease? *J Neuroendocrinol.* 18(9):715-716.
45. Staels B (2006) When the Clock stops ticking, metabolic syndrome explodes. *Nat Med.* 12(1):54-55.
46. Turek FW, *et al.* (2005) Obesity and Metabolic Syndrome in Circadian Clock Mutant Mice. *Science* 308(5724):1043-1045.
47. Bligh EG & Dyer WJ (1959) A rapid method of total lipid extraction and purification. *Can J Biochem Physiol.* 37(8):911-917.
48. Lavery D & Schibler U (1993) Circadian transcription of the cholesterol 7 α hydroxylase gene may involve the liver-enriched bZIP protein DBP. *Genes Dev.* 7(10):1871-1884.

FIGURE LEGENDS

Figure 1: Expression of PPAR α in PAR bZip knockout mice

A. Temporal expression of *Ppar α* mRNA in the livers of wild-type and PAR bZip 3KO mice. RNA levels were estimated by real-time RT-PCR. Mean values \pm SEM obtained from six animals are given.

B. Temporal expression of the PPAR α target genes *Cyp4a10* and *Cyp4a14* in the liver of wild-type and PAR bZip 3KO mice, as determined by real-time RT-PCR. Mean values \pm SEM obtained from six animals are given.

C. Temporal expression of *Ppar α* pre-mRNA transcripts in the livers of wild-type or *Ppar α* KO mice. A PCR amplicon located in the second intron was used in these quantitative RT-PCR experiments. Mean values \pm SEM obtained from four animals are given.

D. Temporal expression of PPAR α protein in liver nuclear extracts from PAR bZip 3KO and wild-type mice. Signals obtained with U2AF⁶⁵ antibody were used as loading controls (U2AF⁶⁵ is a constitutively expressed splicing factor).

E. Ratio of liver PPAR α protein/*Ppar α* mRNA levels after injection of the synthetic PPAR α ligand WY14643 or its solvent (50% DMSO) in PAR bZip 3KO mice at ZT2. Mean values \pm SEM obtained from six animals are given. The raw data used for these computations are presented in Figure S3.

The *Zeitgeber* times (ZT) at which the animals were sacrificed are indicated. * $p \leq 0.05$, ** $p \leq 0.01$ KO vs. WT, Student t-test.

Figure 2: Regulation of the *Acot* genes cluster and lipid metabolizing enzymes in PAR bZip 3KO and *Ppara* KO mice.

A. Organization of the mouse *Acot* gene cluster on chromosome 12. A sequence perfectly matching the PAR bZip consensus binding site is located between *Acot1* and *Acot4*. An

EMSA experiment with liver nuclear extracts from wild-type and PAR bZip 3KO mice shows that PAR bZip transcription factors bind this sequence in a diurnal fashion.

B. Temporal expression of acetyl-CoA Thioesterase (*Acot*) 1 to 4, Lipoprotein Lipase (*Lpl*) and Fatty acid Synthase (*Fasn*) mRNA in PAR bZip 3KO mice. Real time RT-PCR experiments were conducted with whole cell liver RNAs from six animals for each time point. The *Zeitgeber* times (ZT) at which the animals were sacrificed are indicated. Mean values \pm SEM are given. * $p \leq 0.05$, ** $p \leq 0.01$, *** $p \leq 0.001$ KO vs. WT, Student t-test.

C. Expression of *Cyp4a10* and *Cyp4a14* mRNA in mouse liver after treatment with siRNAs directed against *Acot* genes. Real time RT-PCR experiments were conducted with whole cell liver RNAs from four (Control and individual *Acot* siRNA) or six animals (pool of the four precedent *Acot* siRNA). Mean values \pm SEM are given. * $p \leq 0.05$, ** $p \leq 0.005$, Control siRNA vs. *Acot* siRNA, Student t-test.

Figure 3: Lipid metabolism in PAR bZip 3KO mice.

A. Temporal accumulation of FA (C16:0, C18:0, C18:1w7, C18:1w9, C18:2w6 and C20:4w6) in the livers of wild-type and PAR bZip 3KO mice. Mean values \pm SEM obtained from four animals are given. The *Zeitgeber* times (ZT) at which the animals were sacrificed are indicated. Note that the profiles of accumulation are daytime-dependent for all analyzed FA in wild-type animals (ANOVA $F[5,18] = 3.29, 3.72, 9.00, 4.50, 3.86$ and 4.01 and $p \leq 0.05, 0.025, 0.02, 0.015, 0.025$ and 0.025 respectively), whereas they are low and virtually invariable in KO animals. In all the cases, values were statistically different between wild-type and KO animals (ANOVA $F[1,46] = 15.85, 13.11, 10.95, 18.00, 13.96$ and 11.62 , and $p \leq 0.0005, 0.001, 0.0025, 0.0001, 0.001$ and 0.002 , respectively).

B. Serum concentrations of triglycerides, cholesterol, and glucose in wild-type and PAR bZip 3KO animals. Mean values \pm SEM obtained from 12 wild-type and 17 knockout animals are given. For triglycerides, values obtained between ZT4 and ZT14 were separated from the values obtained between ZT16 and ZT2, due to their strong circadian variations. * $p \leq 0.05$, ** $p \leq 0.01$, *** $p \leq 0.001$ KO vs. WT, Student t-test.

Figure 4: Effect of fat free diet on PPAR α target genes expression and serum biochemistry

A. Mice were fed *ad libitum* during five weeks with a fat free diet. For each condition, four mice were sacrificed at ZT0 and ZT12. Total liver RNAs were extracted and analyzed by real time RT-PCR for the expression of mRNAs specified by PPAR α target genes and *Fasn*, a marker gene of lipogenesis that is induced by the fat free diet. # $p \leq 0.05$, ## $p \leq 0.005$, ### $p \leq 0.0005$ fat free vs normal diet in 3KO; § $p \leq 0.05$, §§ $p \leq 0.01$, §§§ $p \leq 0.00005$ fat free vs normal diet in wild-type; * $p \leq 0.05$ KO vs. WT, Student t-test.

B. Serum concentrations of triglycerides, cholesterol and glucose were measured in wild-type and PAR bZip 3KO animals fed with regular or fat free chow. Mean values \pm SEM obtained from eight wild-type and knockout animals are given. For FA, values obtained between ZT4 and ZT14 were separated from the values obtained between ZT16 and ZT2. * $p \leq 0.05$ fat free vs normal diet in 3KO.

Figure 5: Model showing the regulation of PPAR α by metabolism and PAR bZip transcription factors.

Left panel. Under normal diet conditions, the expression of Acetyl-CoA Thioesterases (ACOTs) are under the control of circadian PAR bZip transcription factors. These transcription factors thus control the release of free fatty acid from acyl-coA thioesters, and

the free FA stimulate PPAR α activity. The activated PPAR α then stimulates transcription of *Acot* and *Lpl*, and in a feed-forward loop reinforces its own expression and activity.

Right panel. Under a fat free diet, all free FA are derived from the *de novo* synthesis pathway.

Under these conditions, PPAR α activity is not dependent on PAR bZip transcription factors.

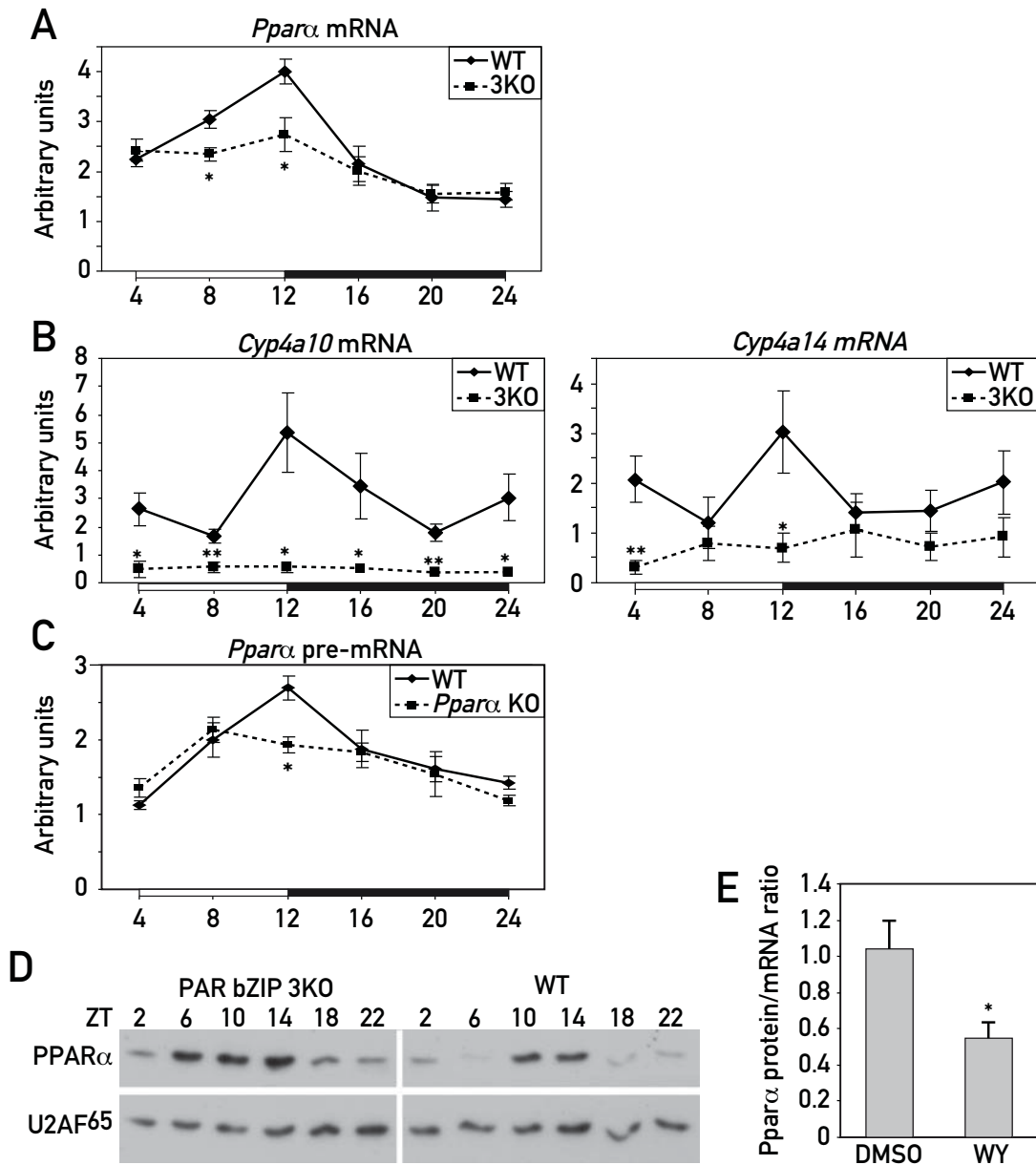


Figure 1

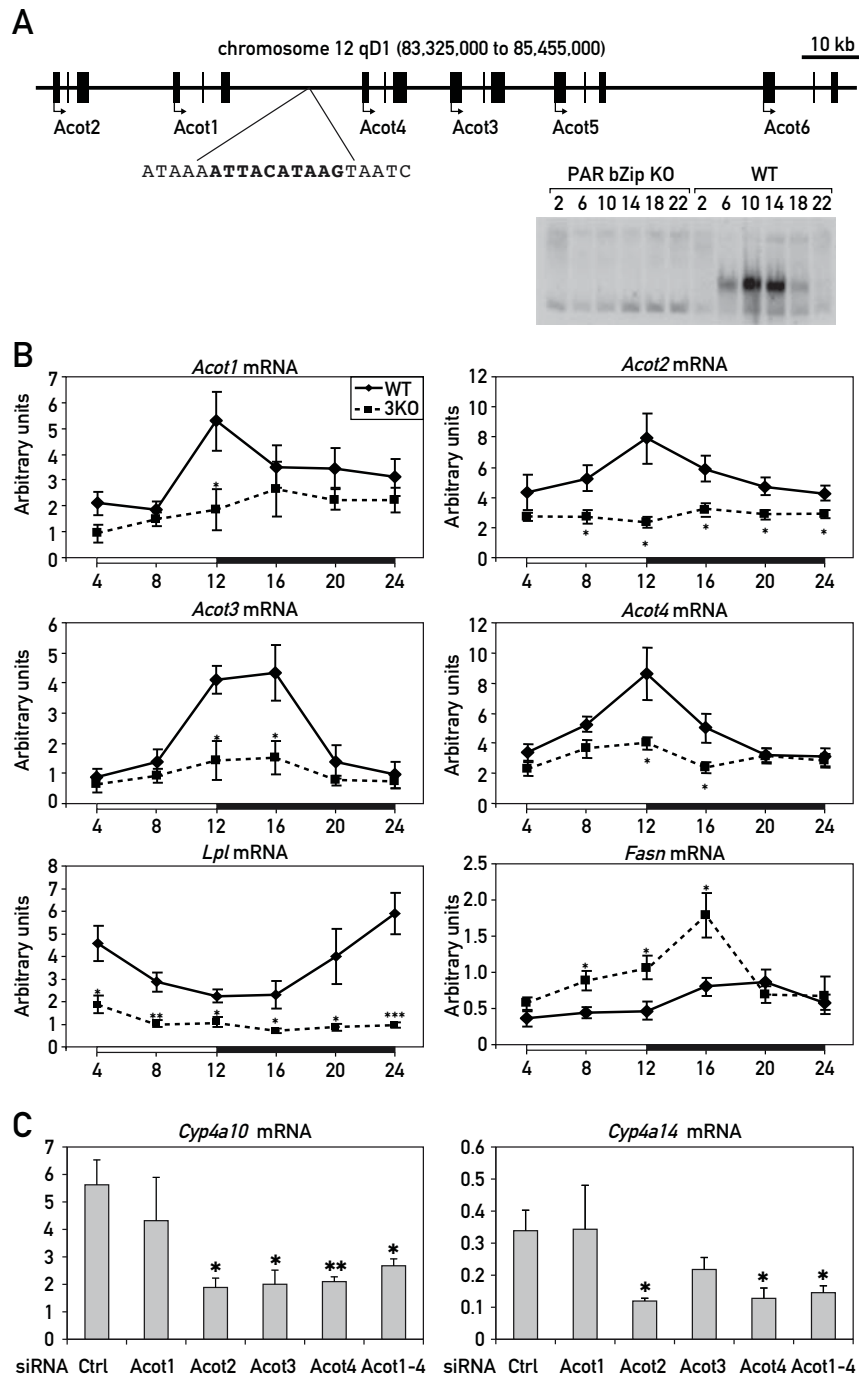


Figure 2

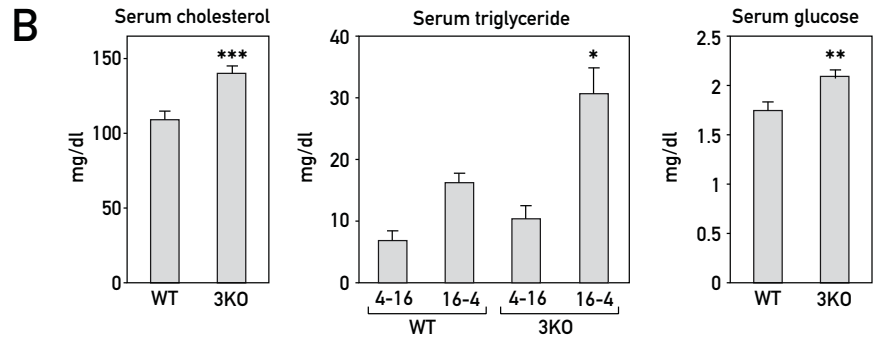
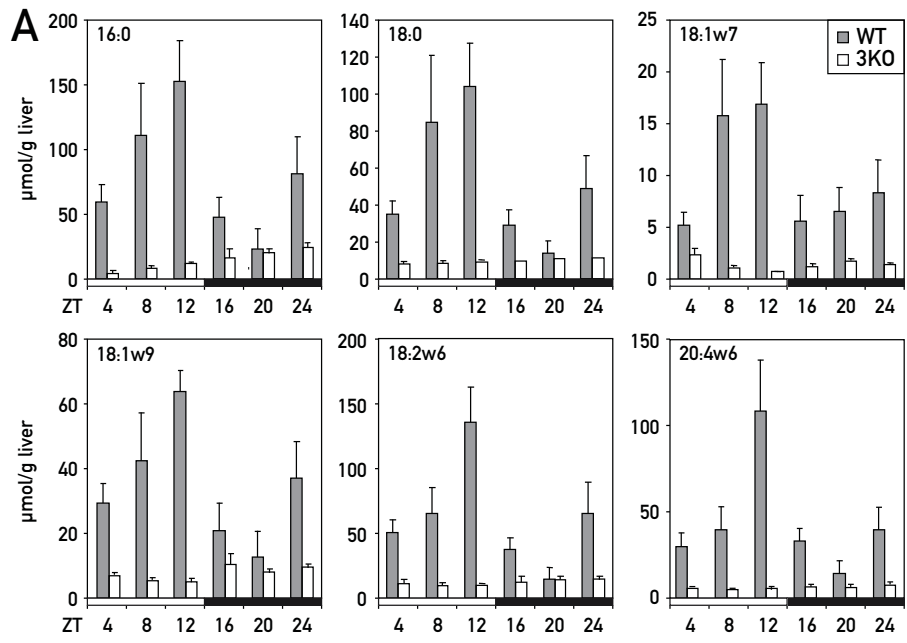


Figure 3

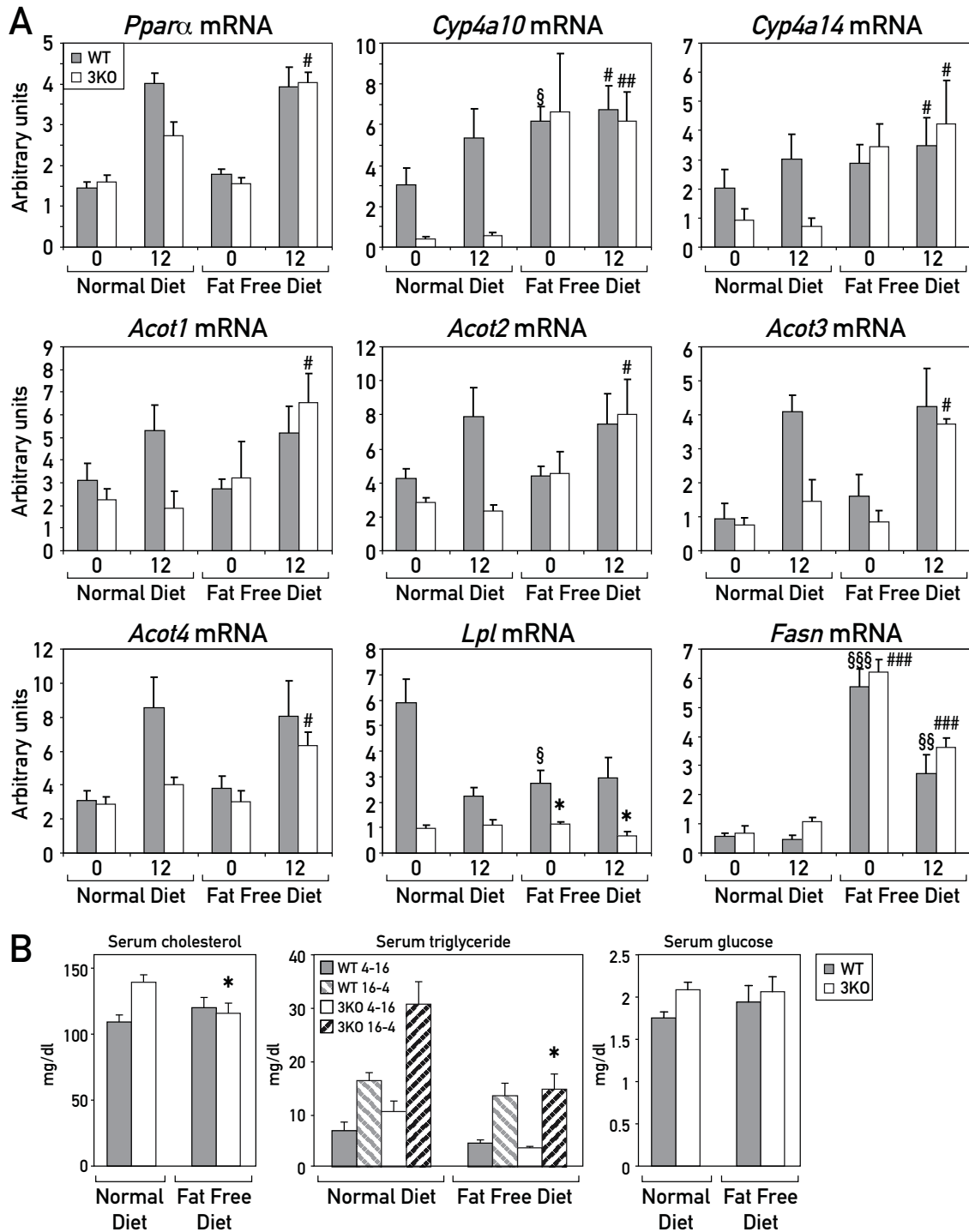


Figure 4

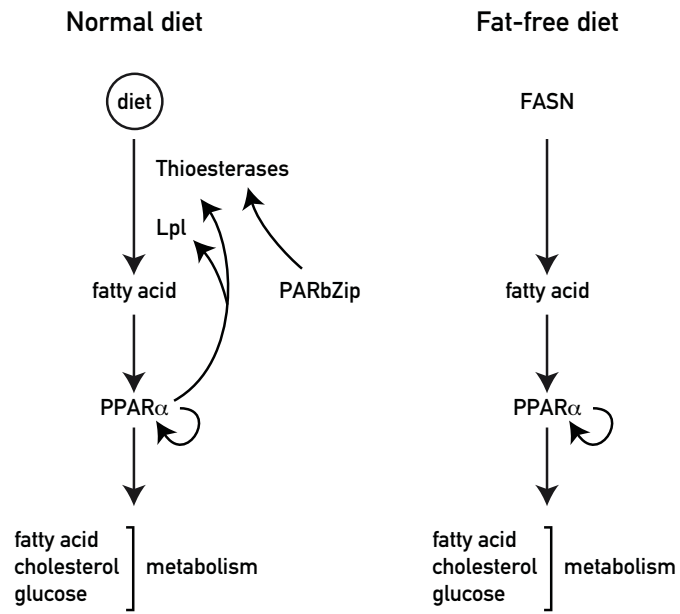


Figure 5

Additional experimental procedures

Animal experiments

WY14643 treatment by intraperitoneal injection. Two groups of 6 PAR bZip 3KO male mice were injected intraperitoneally at ZT2 with 100 mg/Kg WY14643 (Biomol International, Plymouth Meeting, PA) (10 mg/ml in 50% DMSO) or the equivalent volume of vehicle. Four hours after injection, mice were sacrificed and livers were removed and snap-frozen in liquid nitrogen, or immediately processed for the purification of the nuclear proteins used in the immunoblot experiments.

In vivo siRNA treatment. Chemically modified Stealth RNAiTM siRNA duplexes (Invitrogen) complementary to the four *Acots* genes were complexed with InvivoFectamine® 2.0 (Invitrogen) according to manufacturer recommendation before the injection. For each of the four examined *Acots* (*Acots* 1 to 4) six siRNAs with different sequences were tested in two different mice, and the one yielding maximal suppression was selected for the experiments shown in Figures 2C and S9. The sequences of these siRNA are given below. The solution containing control siRNA (a siRNAs with sequences that do not target any gene product that have been tested by microarray analysis and shown to have minimal effects on gene expression), individual *Acot* siRNAs or an equimolar mix of the four *Acot* siRNAs were injected intravenously through the tail vein of 8 week old Balb/c mice at ZT12 at a dose of 7 mg/kg. 48 hours after the injection, mice were sacrificed and livers were removed and snap-frozen in liquid nitrogen, and stored at -70 °C before RNA was extracted.

Calorie Restriction. PAR bZip 3KO mice and wild-type siblings (9 knockouts and 7 wild-type 7 to 9 weeks male mice) were fed regular chow (ref 3800 from Provimi Kliba, Switzerland. Diet composition: 24 % protein, 47.5 % carbohydrate, 4.9 % fat) *ad libitum* for at least three months. Mice were then separated (by placing them into individual cages) and fed with powdered food that was delivered by a computer-driven feeding machine (1). Average food consumption was determined to be 4.2 g/day/mouse for animals fed *ad libitum* with regular chow, and this value was used as the normal diet control value in the caloric restriction studies. The animals were then subjected to a calorie diet reduced by 40% (i.e. 2.52 g/day/animal distributed into 20 daily portions delivered every 30 min between ZT12 and ZT22). The animals were weighed twice a week in the morning for 11 weeks.

Temporally restricted feeding. 3.4 g of powdered chow (80% of the normal diet control value) were offered in 12 portions between ZT03 and ZT09 by a computer-driven feeding machine (1). The wheel-running activities of the animals were recorded as described previously (2).

Fat-free feeding regimen. 8 week old PAR bZip 3KO mice and wild-type siblings (4 males and 4 females of each genotype) were fed with regular chow *ad libitum* for at least three months. The food was then replaced by a fat free diet (TD.03314 from Harlan Teklad, Madison, WI. Diet composition: 20.1 % protein, 62.9 % carbohydrate, 0 % fat) for 5 weeks.

Electromobility shift assay

The radio-labeled probe was prepared by annealing two oligonucleotides encompassing the PAR bZip binding site present in the *Acot* genes cluster and by filling in the 5' overhang with [α -

³²P].dCTP and Klenow DNA polymerase. The sequences of these oligonucleotides were 5'-CCATAAAATTACATAAG-3' and 5'-TTGATTACTTATGTAATTTTATGG-3'. Twenty micrograms of liver nuclear extract were incubated with 100 fmoles of the double-stranded oligonucleotide in a 20 µl reaction containing 25 mM HEPES (pH 7.6), 60 mM KCl, 5 mM MgCl₂, 0.1 mM EDTA, 7.5% glycerol, 1 mM DTT, 1 µg/µl salmon sperm DNA. After an incubation of 10 min at room temperature, 2 µl of a 15% Ficoll solution were added, and the protein-DNA complexes were separated on a 5% polyacrylamide gel in 0.25 x TBE.

GC-MS determination of fatty acids concentrations

Lipid extracts were taken to dryness in a speed-vac evaporator and resuspended in 240 µl of 50% weight/volume KOH and 800 µl ethanol for the alkaline hydrolysis of lipids. After a 60 min incubation at 75°C, FA were extracted with 1 ml of water and 2 ml of hexane. The hexane phase was taken to dryness and redissolved in 50 µl of a pentafluoro-benzyl bromide solution (3.4 % in acetonitrile) and 10 µl of N,N-diisopropyl ethanolamine. After 10 min of incubation at room temperature, samples were evaporated under a gentle stream of nitrogen and resuspended in 50 µl of hexane.

A Trace-DSQ GC-MS (Thermo Scientific, Austin, TX) equipped with a TR5MS 30m column was used for the mass-spectrometric analysis of lipids by gas chromatography. Helium was used as carrier gas at 1 ml/min in splitless mode at 300°C injector temperature. The initial oven temperature of 150°C was held for 1min and then the temperature first was ramped up to 200°C at a rate of 25°C/min. This was followed by a ramp of 12.5°C/min up to 325°C, where the temperature was held for another 2min. The mass spectrometer was run in negative ion chemical ionization (NICI) mode where the FAs were detected in full scan as carboxylates after loss of the

pentafluoro benzyl moiety. Methane was used as CI gas, the source temperature was set to 250°C and the transfer line temperature was 330°C. Peak areas for FA were calculated by Xcalibur QuanBrowser and related to the internal standard peak area.

Sequences of the primers used for Real-time PCR

Gene	Forward primer	Reverse primer
<i>Pparα</i> intron 1	TGGCCCCAACAGTAGGGTAG	TGGAGGGCAGAGACATAGGG
<i>Cyp4a10</i>	GGAGCTCCAATGTCTGAGAAGAGT	TCTCTGGAGTATTCTTCTGAAAAAGGT
<i>Cyp4a14</i>	TCTCTGGCTTTTCTGTACTTTGCTT	CAGAAAGATGAGATGACAGGACACA
<i>Acot1</i>	GACTGGCGCATGCAGGAT	CCAGTTTCCATAGAACGTGCTTT
<i>Acot2</i>	CAAGCAGGTTGTGCCAACAG	GAGCGGCGGAGGTACAAAC
<i>Acot3</i>	GGTGGGTGGTCCTGTCATCT	TGTCTTCTTTTTTGCCATCCAAAT
<i>Acot4</i>	GGCCTTGAACTCACAGGGATT	AGGTAGGGCCGAGCCTTTAA
<i>Acox1</i>	GGATGGTAGTCCGGAGAACA	AGTCTGGATCGTTCAGAATCAAG
<i>Acaab1</i> (<i>Thiolase B</i>)	TCCAGGACGTGAAGCTAAAGC	CATTGCCACGGAGATGTC
<i>Cpt1</i>	CCTGGGCATGATTGCAAAG	ACGCCACTCACGATGTTCTTC
<i>Acadm</i> (<i>Mcad</i>)	AGCTGCTAGTGGAGCACCAAG	TCGCCATTTCTGCGAGC
<i>Fabp1</i> (<i>L-Fabp</i>)	CCAGGAGAACTTTGAGCCATTC	TGTCCTTCCCTTTCTGGATGA
<i>Cd36</i>	GATGACGTGGCAAAGAACAG	TCCTCGGGGTCCTGAGTTAT
<i>Srebp2</i>	GCGTTCTGGAGACCATGGA	ACAAAGTTGCTCTGAAAACAAATCA
<i>Ldlr</i>	TGGGCTCCATAGGCTATCTG	GCCACCACATTCTTCAGGTT

For the other genes, we used the following designed primers from Applied Biosystems:

Gapdh	Mm99999915_g1
Pparα	Mm00440939_m1
Lpl	Mm00434770_m1
Fasn	Mm01253300_g1

Sequences of *Acot* siRNA

Gene	Sequence
<i>Acot1</i>	AGCUCUUCUUGUCUACCAGAGGGCU
<i>Acot2</i>	CCCAAGAGCAUAGAAACCAUGCACA
<i>Acot3</i>	GAACCCGAACCGGAUGGCACCUACU
<i>Acot4</i>	CAACGUCAUAGAAGUGGACUACUUU

Legends to Supplemental Figures

Figure S1: Hepatic expression of PPAR α target genes in PAR bZip 3KO mice.

A. Microarray data obtained with PAR bZip 3KO mouse liver RNA (3) were compared to data obtained with *Ppara* KO mouse liver RNA (4). Genes downregulated in both genotypes with regard to their wild-type counterparts are listed. The table corresponds to the list of genes downregulated more than 1.25-fold in at least one of the knockout genotypes (when compared to strain-matched wild-type mice).

B. Temporal hepatic expression of genes coding for enzymes involved in peroxisomal fatty acid β -oxidation [Acyl-CoA oxidase 1 (*Acox1*) and Acyl-CoA acyltransferase 1B or Thiolase B (*Acaal1b*)], mitochondrial fatty acid β -oxidation [Carnitine palmitoyltransferase 1 (*Cpt1*) and Mitochondrial medium-chain acyl-CoA dehydrogenase or MCAD (*Acadm*)] and fatty acid binding and transport (fatty acid-binding protein 1 or L-FABP (*Fabp1*) and CD36 (*Cd36*)] in wild-type and PAR bZip 3KO mice, as determined by real-time RT-PCR. Mean values \pm SEM obtained from four animals are given.* $p \leq 0.05$, ** $p \leq 0.01$, KO vs. WT, Student t-test.

As for *Cyp4a* genes, the PPAR α target genes coding for enzymes involved in fatty acid β -oxidation are also downregulated [*Acox1*, *Acaal1b* (see also figure S1A for these genes) and *Cpt1*] or not changed (*Acadm*) in the liver of PAR bZip 3KO mice. Interestingly, the genes coding for proteins involved in the fatty acid transport exhibit an increased expression in PAR bZip 3KO mice, confirming previously published microarray data (3). Similar to what has been observed for *Fasn* expression, the increased expression of these genes is probably an indirect consequence of the disrupted fatty acid metabolism in PAR bZip 3KO mice, perhaps to compensate for the deficient import and/or metabolism of lipids absorbed with the food.

Figure S2: Temporal expression of the PPAR α target genes *Cyp4a10* and *Cyp4a14* in the liver of *Ppar α* KO and wild-type mice.

- A. Temporal expression of *Cyp4a10* and *Cyp4a14* in the liver of wild-type and *Ppar α* KO mice.
- B. Temporal expression of acetyl-CoA Thioesterase (*Acot*) 1 to 4, Lipoprotein Lipase (*Lpl*) and Fatty acid Synthase (*Fasn*) mRNA in wild-type and *Ppar α* KO mice.

Real time RT-PCR experiments were conducted with whole cell liver RNAs from four animals for each time point. The *Zeitgeber* times (ZT) at which the animals were sacrificed are indicated. Mean values \pm SEM obtained from four animals are given.* $p \leq 0.05$, ** $p \leq 0.01$, *** $p \leq 0.001$ KO vs. WT, Student t-test.

Figure S3: PPAR α protein/mRNA ratio after the activation of PPAR α by its synthetic ligand WY14643.

Six PAR bZip 3KO mice were injected intraperitoneally (i.p.) with DMSO (left panel) or PPAR α ligand WY14643 (100 mg/kg) at ZT2. Livers were harvested four hours later, and nuclear proteins and whole cell RNAs were extracted. The PPAR α protein levels were quantified by western blot experiments (upper panel), and *Ppar α* mRNA was quantified by real time RT-PCR (middle panel). Individual ratios between liver PPAR α protein and *Ppar α* mRNA are plotted in the bottom panel. The mean values \pm SEM are given in Figure 1E.

Figure S4: Activation of hepatic *Cyp4a*, *Acots* and *Lpl* expression after injection of the PPAR α activator WY14643.

Six PAR bZip 3KO male mice were injected i.p. with DMSO or PPAR α ligand WY14643 (100 mg/kg) at ZT2. Livers were harvested four hours later, and whole cell RNAs were extracted. mRNAs of the indicated genes were quantified by real time RT-PCR. Mean values \pm SEM are given.* $p \leq 0.05$, ** $p \leq 0.005$, *** $p \leq 0.0005$ DMSO vs. WY14643 injection, Student t-test.

Figure S5: Response of PAR bZip 3KO mice to caloric restriction

Wild-type (black line) and PAR bZip 3KO (dotted line) animals were fed with a diet containing only 60% of the normal calorie consumption during eleven consecutive weeks. Animals were weighted twice a week during this period. Mean relative weight changes \pm SEM obtained from seven wild-type and nine knockout animals are given.

Figure S6: PAR bZip 3KO mice display normal O₂ consumption and CO₂ production

Oxygen consumption (VO₂) and carbon dioxide production (VCO₂) were measured by indirect calorimetry with the Comprehensive Lab Animal Monitoring System (CLAMS) (Columbus Instruments, Columbus, OH). After three days of accommodation, VO₂ (A) and VCO₂ (B) were recorded during a 24 hours period. Mean values \pm SD obtained from four animals of each genotype are given.

Figure S7: Food anticipatory activities (FAA) of wild-type, PAR bZip 3KO, and *Ppar α* KO mice

A. Examples of FAA recordings of wild-type (left panel) and PAR bZip 3KO (right panel) mice. Animals received 80% of their normal food consumption between ZT3 and ZT9 for the duration of the experiment.

B. Percentage mean activity during a 24-hour period for animals subjected to temporally restricted feeding. Mean values \pm SEM obtained from four animals of each genotype (recorded between day 10 and day 20 after the onset of restricted feeding) are given. The areas under which values are significantly different (Student's *t* test p values ≤ 0.05) between PAR bZip 3KO and wild-type mice are indicated by black lines on top of the figure.

C. Examples of FAA of wild-type (left panel) and *Ppar α* KO (right panel) mice. Animals received 80% of their normal food consumption between ZT3 and ZT9 for the duration of the experiment.

Figure S8: Liver fatty acid levels in mice exposed to a fat free diet.

Concentrations of fatty acids (C16:0, C18:0, C18:1w9, C18:1w11, C18:2 and C20:4) in the liver of wild-type and PAR bZip 3KO mice at ZT0 and ZT12. Mean values \pm SEM obtained for four animals are given. In none of the cases did we detect statistically different values with regard to either daytime or genotype.

Figure S9: Effect of ACOT siRNA on *Acot* genes and non-PPAR α regulated genes expression.

A. Accumulation of *Acot* mRNAs in mouse liver 48 hours after the treatment with siRNA directed against *Acot* genes. siRNAs act mainly by decreasing the levels of their target mRNA (5), and the cellular concentrations of *Acot1*, *Acot2*, and *Acot4* mRNA were indeed reduced to 10% to 50% after the injection of their respective siRNAs. None of the six examined *Acot3* siRNAs (see additional experimental procedures) reduced its target mRNA significantly, yet three of them did lower the expression of the PPAR α target genes *Cyp4a10* and *Cyp4a14*. A

similar observation was made for the mix of the four *Acot* siRNAs. Indeed, it has recently been shown that siRNAs, similar to miRNAs, can also act by inhibiting translation of their target mRNA, without reducing the levels of their target mRNAs (6, 7). This phenomenon could explain the observation that *Acot3* siRNA and the mix of the four *Acot* siRNAs strongly reduced the expression of *Cyp4a10* and *Cyp4a14*.

B. Expression of genes involved in lipid metabolism (*Srebp2* and *Ldlr*), two transcripts whose levels were similar in wild-type and PPAR α or PAR bZip triple knockout mice (3, 8, 9). Note that neither individual *Acot* siRNAs nor the mix of the four *Acot* siRNAs significantly affected the accumulation of *Srebp2* and *Ldlr* mRNAs. These results support the specificity of the effect of the *Acot* siRNAs for PPAR α target genes.

Real time RT-PCR experiments were conducted with whole cell liver RNAs from four (Control and individual *Acot* siRNAs) or six animals (pool of the four precedent *Acot* siRNAs). Mean values \pm SEM are given. * $p \leq 0.05$, ** $p \leq 0.01$, *** $p \leq 0.001$ Control siRNA vs. *Acot* siRNAs, Student t-test.

References

1. van der Veen DR, *et al.* (2006) Impact of behavior on central and peripheral circadian clocks in the common vole *Microtus arvalis*, a mammal with ultradian rhythms. *Proc Natl Acad Sci U S A* 103(9):3393-3398.

2. Lopez-Molina L, Conquet F, Dubois-Dauphin M, & Schibler U (1997) The DBP gene is expressed according to a circadian rhythm in the suprachiasmatic nucleus and influences circadian behavior. *EMBO J.* 16(22):6762-6771.
3. Gachon F, Fleury Olela F, Schaad O, Descombes P, & Schibler U (2006) The circadian PAR-domain basic leucine zipper transcription factors DBP, TEF, and HLF modulate basal and inducible xenobiotic detoxification. *Cell Metab.* 4(1):25-36.
4. Leuenberger N, Pradervand S, & Wahli W (2009) Sumoylated PPAR α mediates sex-specific gene repression and protects the liver from estrogen-induced toxicity in mice. *J Clin Invest* 119(10):3138-3148.
5. Guo H, Ingolia NT, Weissman JS, & Bartel DP (2010) Mammalian microRNAs predominantly act to decrease target mRNA levels. *Nature* 466(7308):835-840.
6. Davidson TJ, *et al.* (2004) Highly Efficient Small Interfering RNA Delivery to Primary Mammalian Neurons Induces MicroRNA-Like Effects before mRNA Degradation. *J Neurosci.* 24(45):10040-10046.
7. Tang G (2005) siRNA and miRNA: an insight into RISCs. *Trends Biochem Sci.* 30(2):106-114.
8. Knight BL, *et al.* (2005) A role for PPAR α in the control of SREBP activity and lipid synthesis in the liver. *Biochem J* 389(2):413-421.
9. Patel DD, Knight BL, Wiggins D, Humphreys SM, & Gibbons GF (2001) Disturbances in the normal regulation of SREBP-sensitive genes in PPAR α -deficient mice. *J. Lipid Res.* 42(3):328-337.

A

Affy ID	Gene Symbol	Description	PPAR α KO	PARbZip 3KO
1424853_s_at	Cyp4a10	cytochrome P450, family 4, subfamily a, polypeptide 10	-61.23	-6.03
1423257_at	Cyp4a14	cytochrome P450, family 4, subfamily a, polypeptide 14	-32.25	-2.73
1424716_at	Retsat	retinol saturase (all trans retinol 13,14 reductase)	-4.49	-1.9
1419430_at	Cyp26a1	cytochrome P450, family 26, subfamily a, polypeptide 1	-4.12	-1.98
1424715_at	Retsat	retinol saturase (all trans retinol 13,14 reductase)	-3.88	-1.82
1440134_at	Cyp4a10	cytochrome P450, family 4, subfamily a, polypeptide 10	-3.65	-1.75
1448080_at	E2f8	E2F transcription factor 8	-3.44	-7.28
1448491_at	Ech1	enoyl coenzyme A hydratase 1, peroxisomal	-3.20	-1.35
1428223_at	Mfsd2	major facilitator superfamily domain containing 2	-3.11	-1.48
1451084_at	Etfhd	electron transferring flavoprotein, dehydrogenase	-2.57	-1.31
1421011_at	Dhrs8	dehydrogenase/reductase (SDR family) member 8	-2.49	-1.61
1431833_a_at	Hmgcs2	3-hydroxy-3-methylglutaryl-Coenzyme A synthase 2	-2.49	-1.23
1424451_at	Acaa1b	acetyl-Coenzyme A acyltransferase 1B	-2.45	-1.37
1423858_a_at	Hmgcs2	3-hydroxy-3-methylglutaryl-Coenzyme A synthase 2	-2.30	-1.21
1421430_at	Rad51l1	RAD51-like 1 (<i>S. cerevisiae</i>)	-2.18	-2.44
1416946_a_at	Acaa1b	acetyl-Coenzyme A acyltransferase 1B	-2.17	-1.27
1416947_s_at	Acaa1b	acetyl-Coenzyme A acyltransferase 1B	-2.14	-1.21
1454159_a_at	Igfbp2	insulin-like growth factor binding protein 2	-2.13	-1.5
1449051_at	Ppara	peroxisome proliferator activated receptor alpha	-2.06	-1.55
1434642_at	Dhrs8	dehydrogenase/reductase (SDR family) member 8	-1.83	-1.28
1422526_at	Acs1l	acyl-CoA synthetase long-chain family member 1	-1.70	-1.22
1415776_at	Aldh3a2	aldehyde dehydrogenase family 3, subfamily A2	-1.63	-1.29
1450643_s_at	Acs1l	acyl-CoA synthetase long-chain family member 1	-1.61	-1.27
1415965_at	Scd1	stearoyl-Coenzyme A desaturase 1	-1.56	-1.49
1418989_at	Ctse	cathepsin E	-1.54	-1.56
1438055_at	Rarres1	retinoic acid receptor responder (tazarotene induced) 1	-1.51	-1.44
1423883_at	Acs1l	acyl-CoA synthetase long-chain family member 1	-1.49	-1.23
1415964_at	Scd1	stearoyl-Coenzyme A desaturase 1	-1.42	-1.45
1422032_a_at	Za20d3	zinc finger, A20 domain containing 3	-1.42	-1.37
1416409_at	Acox1	acyl-Coenzyme A oxidase 1, palmitoyl	-1.39	-1.25
1427229_at	Hmgcr	3-hydroxy-3-methylglutaryl-Coenzyme A reductase	-1.34	-1.47
1418654_at	Hao3	hydroxyacid oxidase (glycolate oxidase) 3	-1.27	-1.3
1424493_s_at	Ugt3a1	UDP glycosyltransferases 3 family, polypeptide A1	-1.25	-1.29
1416933_at	Por	P450 (cytochrome) oxidoreductase	-1.23	-1.41

B

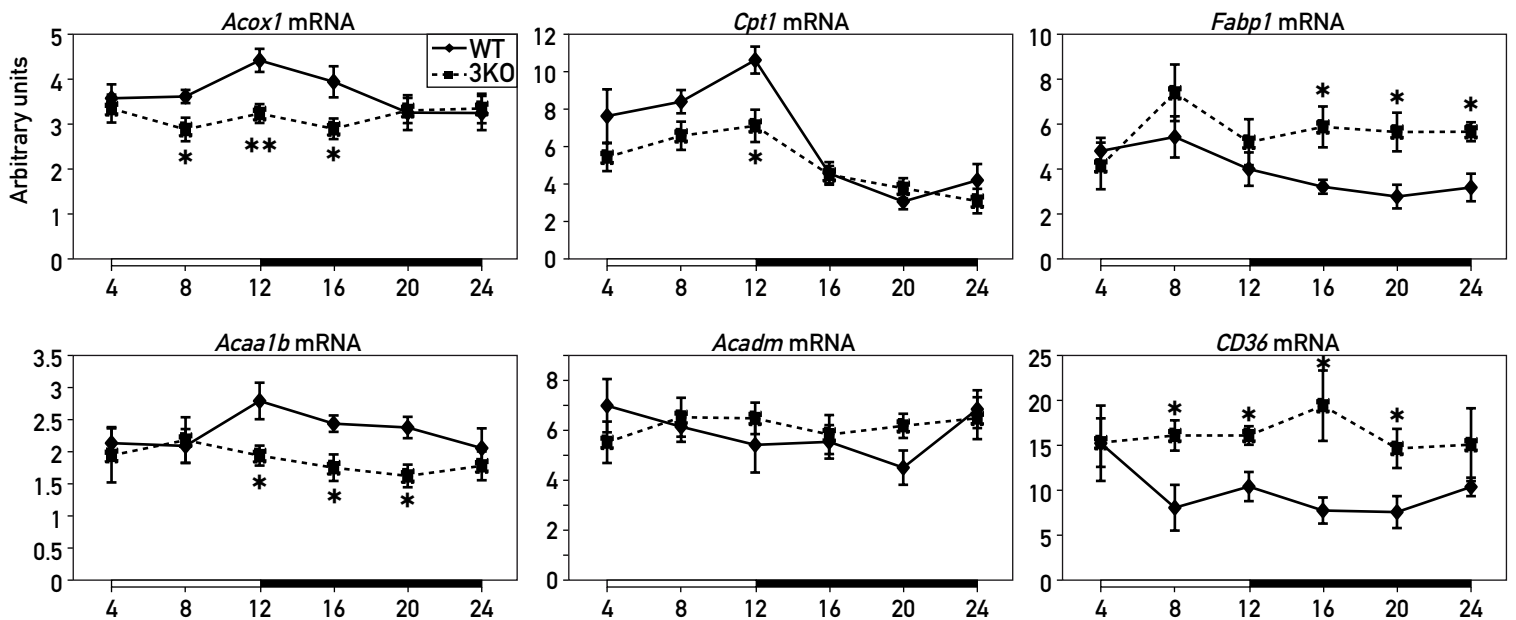


Figure S1

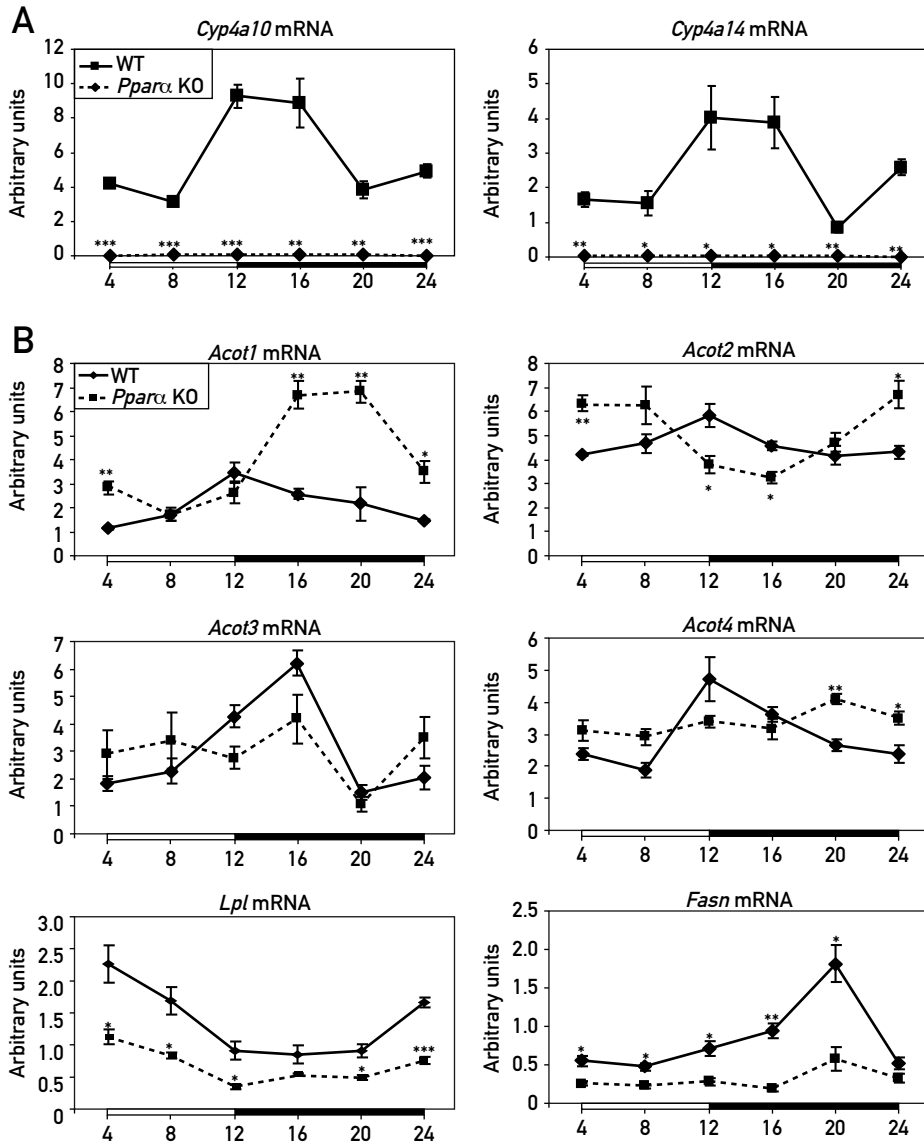


Figure S2

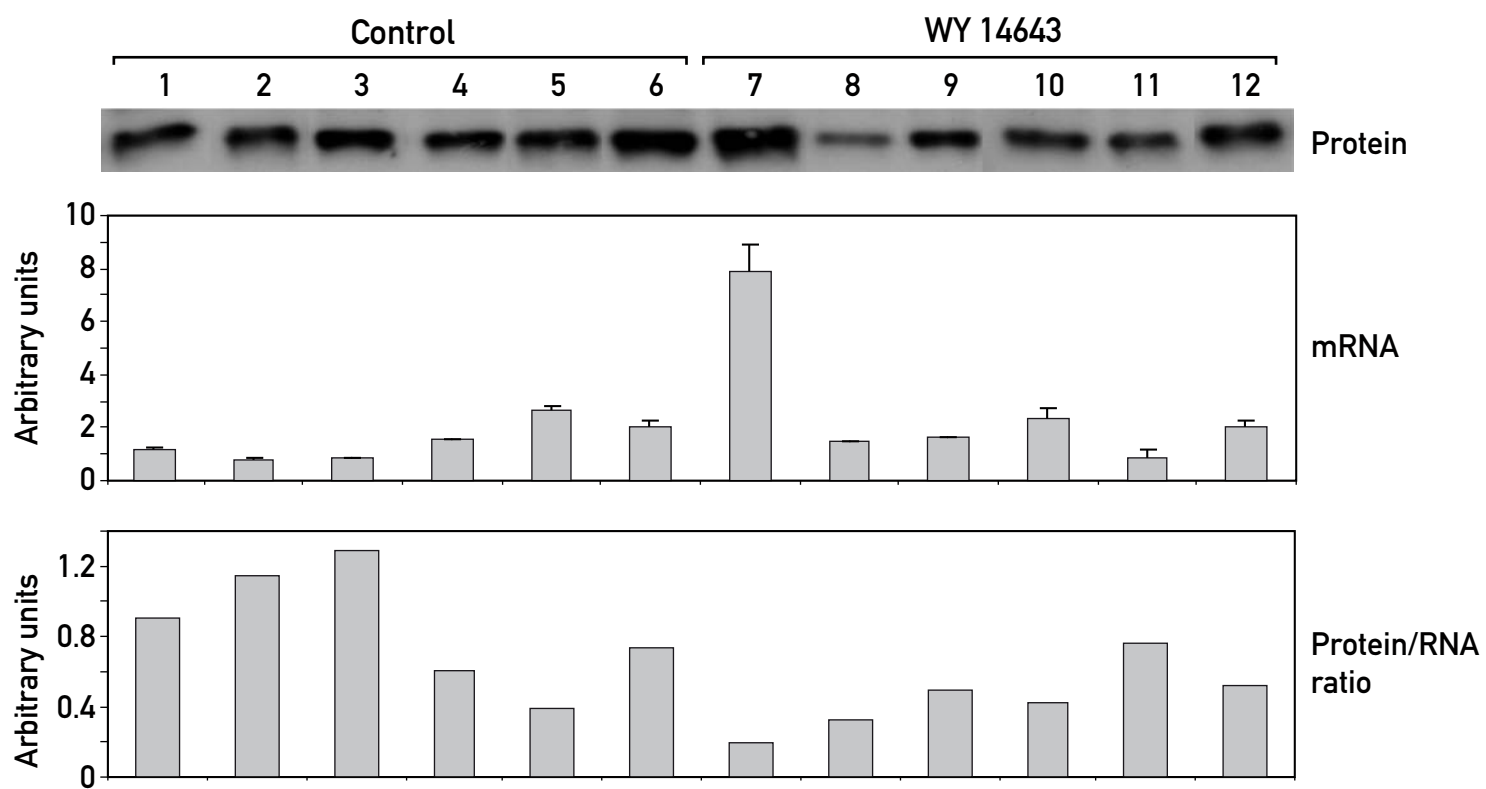


Figure S3

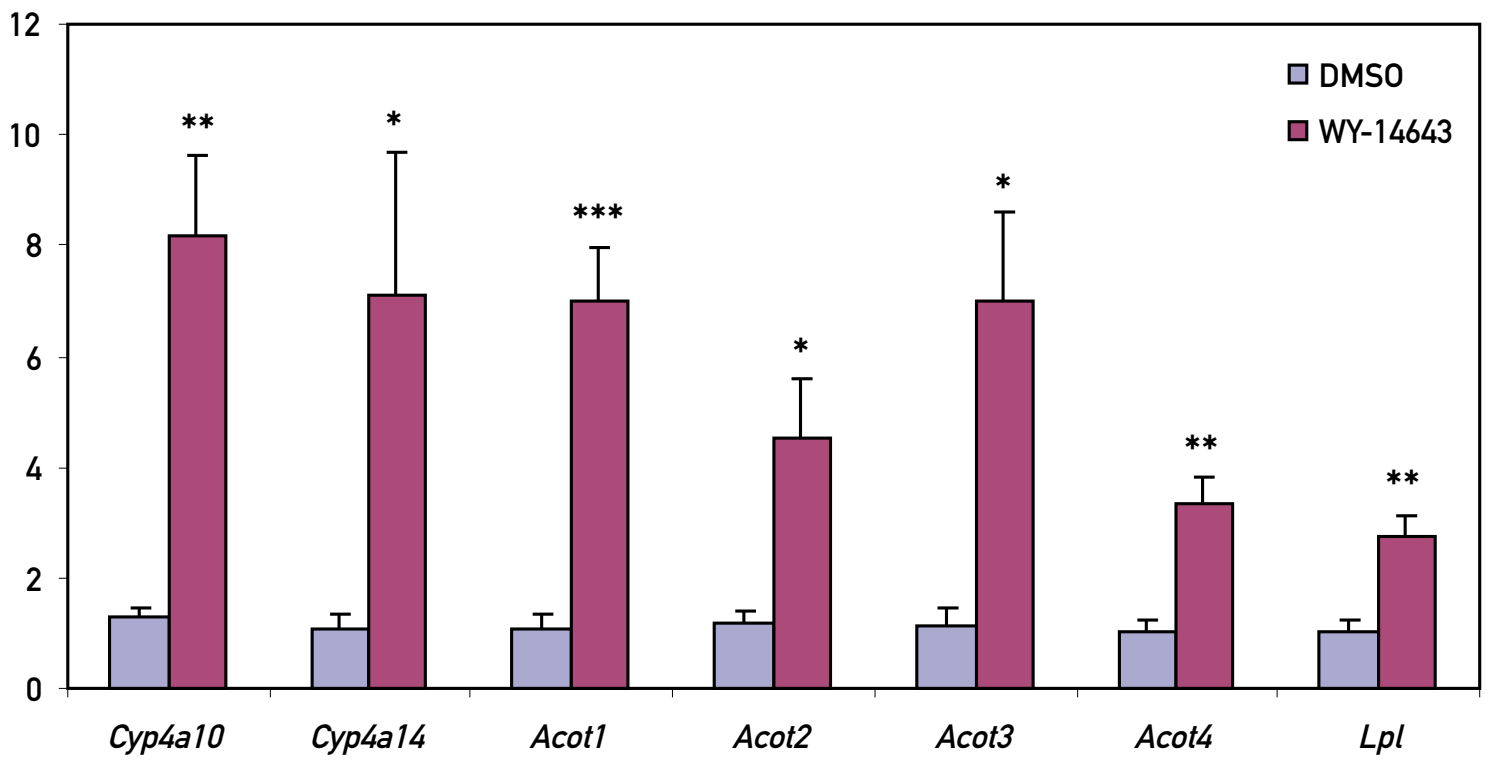


Figure S4

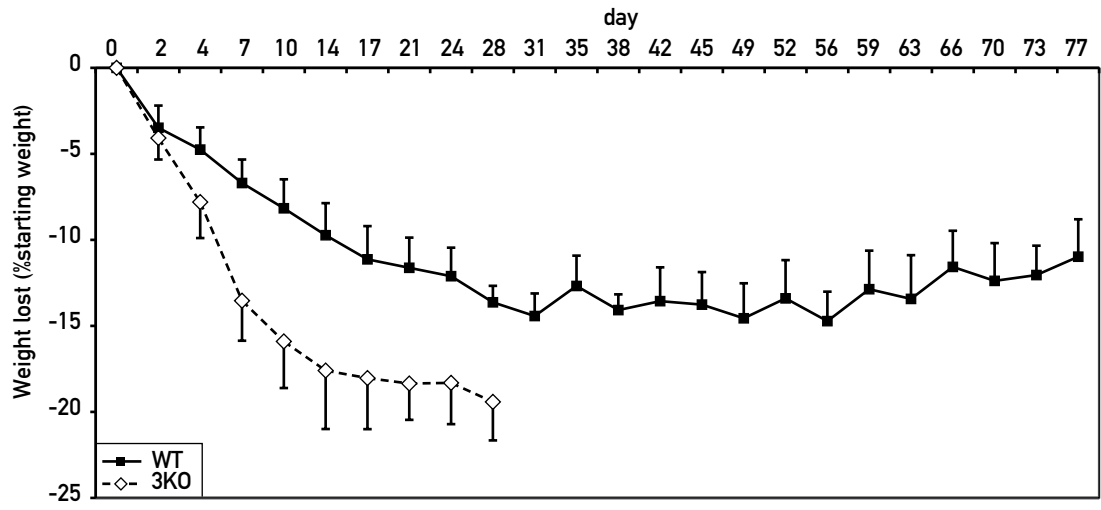


Figure S5

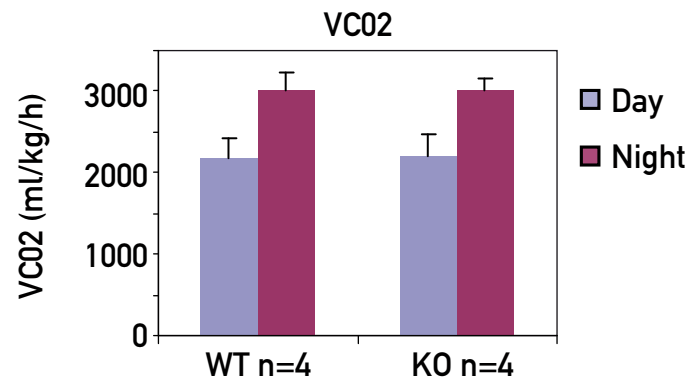
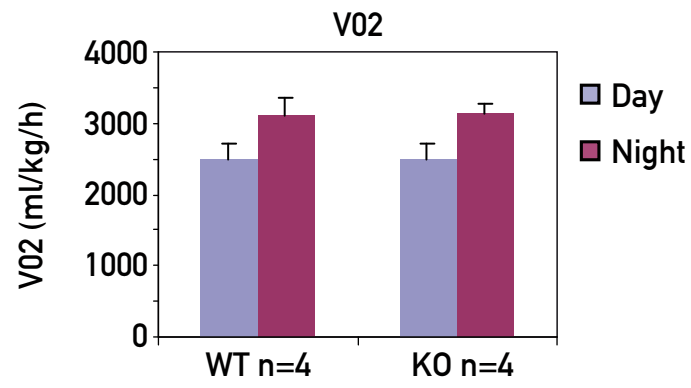


Figure S6

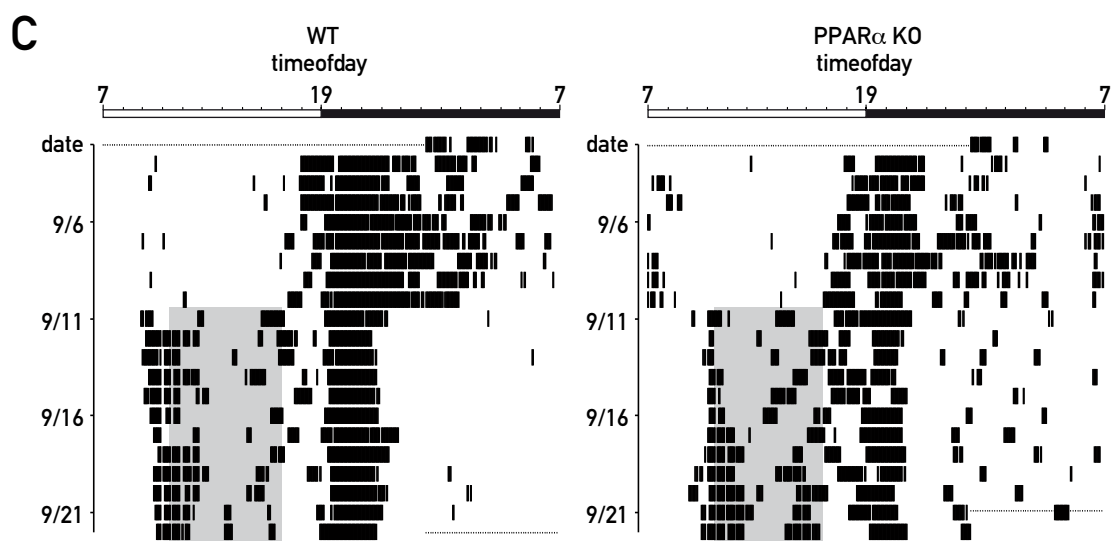
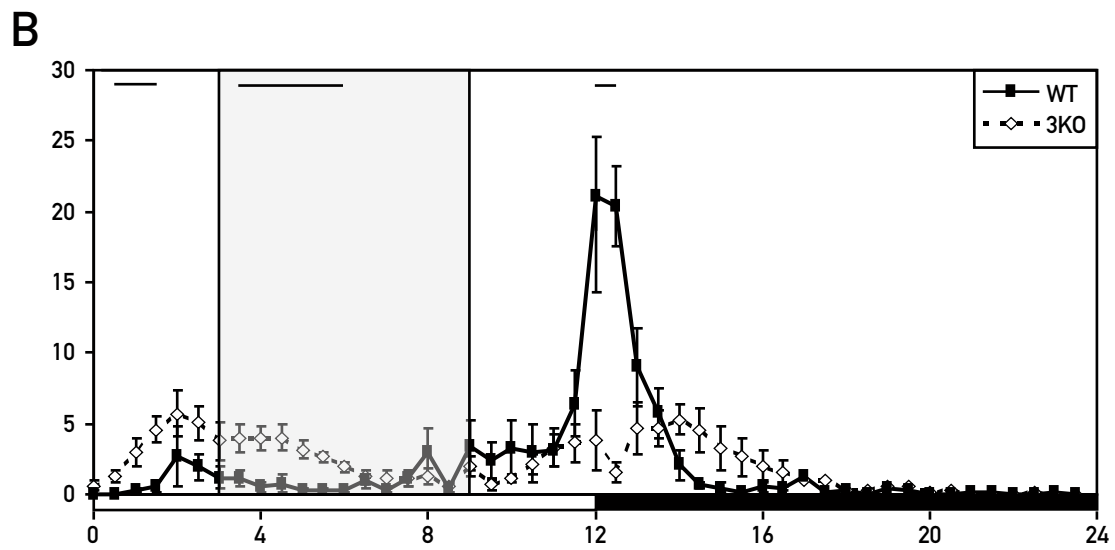
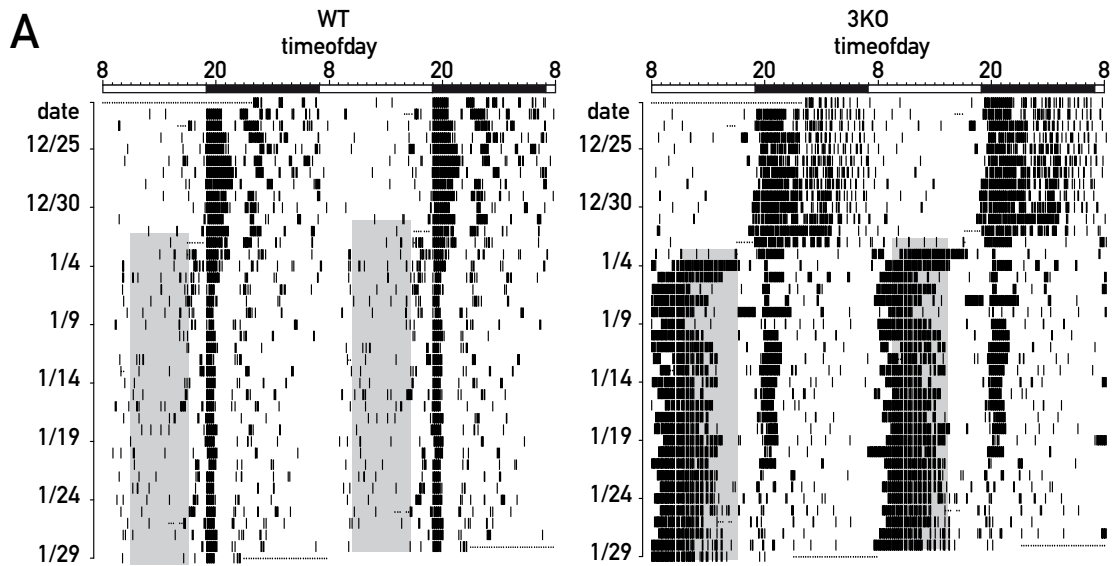


Figure S7

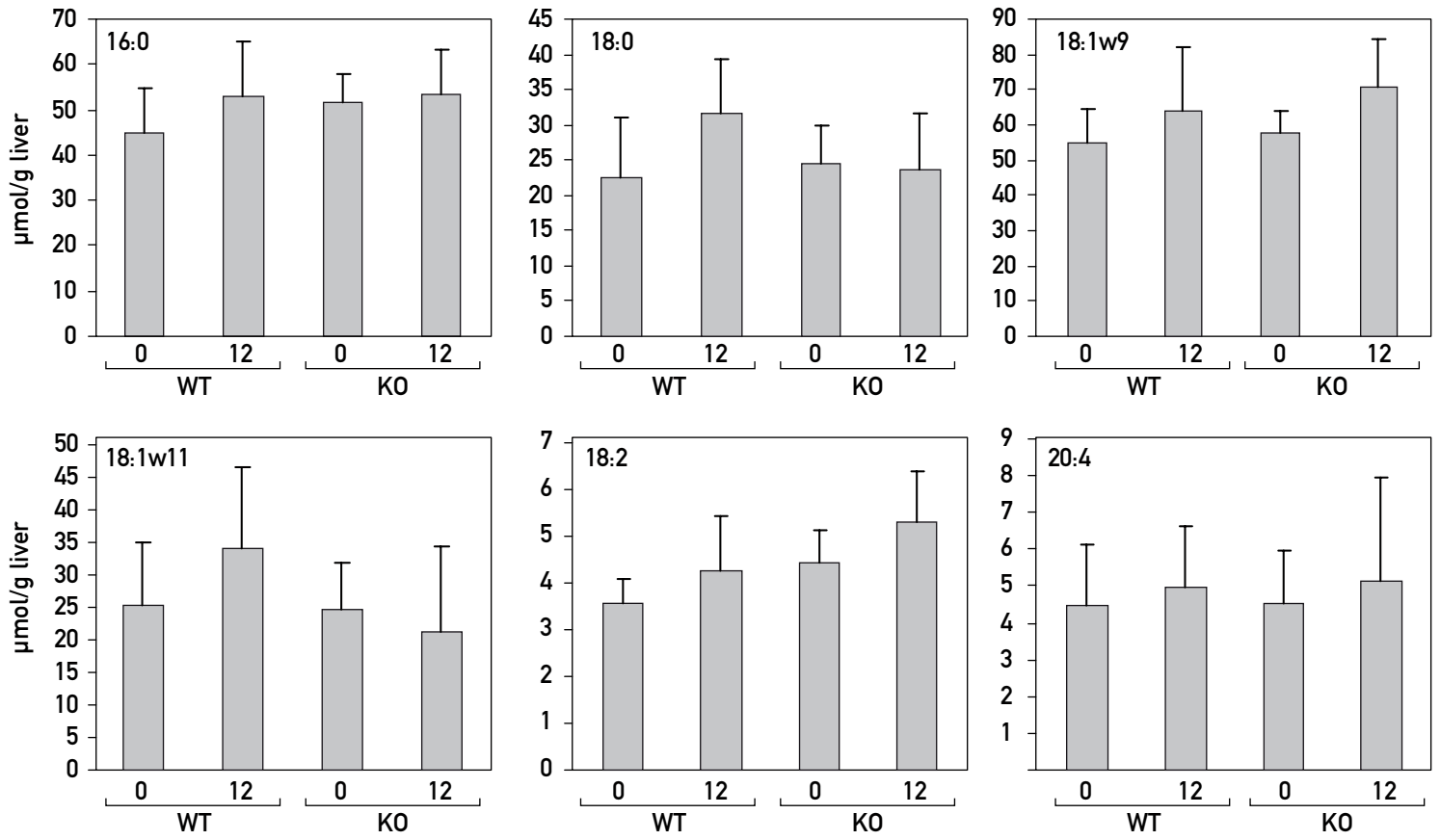


Figure S8

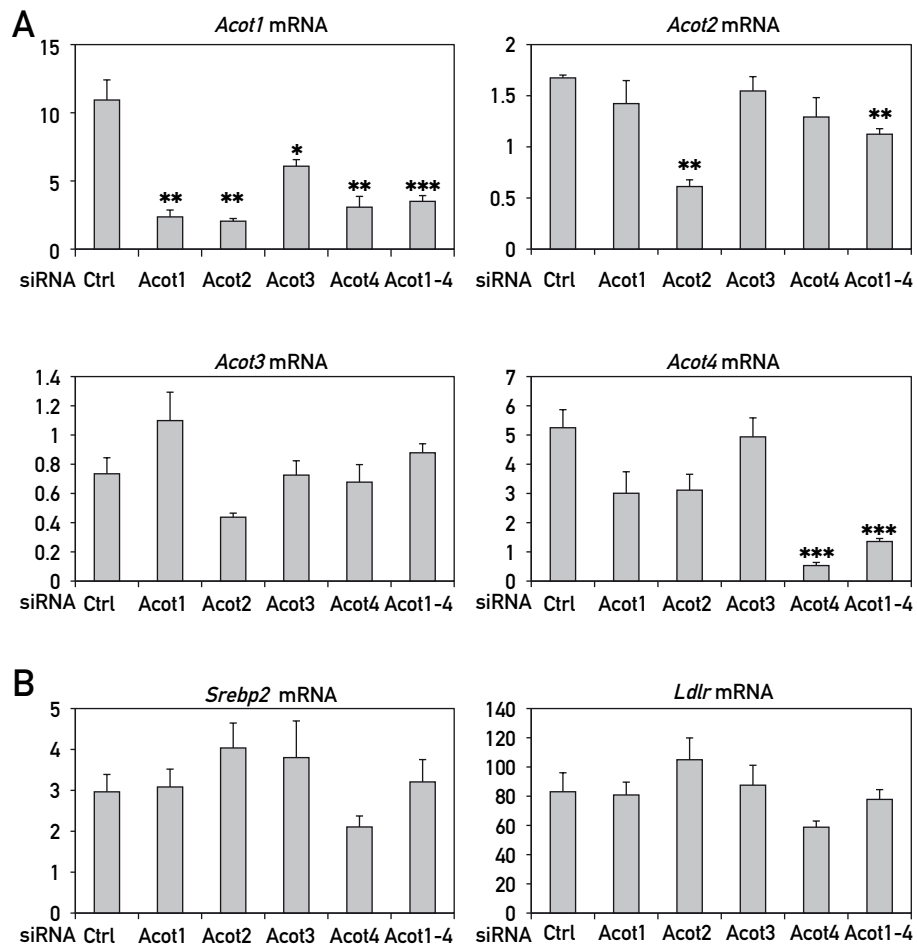


Figure S9